Quaternary Science Reviews 78 (2013) 77–97

Contents lists available at ScienceDirect

Quaternary Science Reviews

journal homepage: www.elsevier.com/locate/quascirev

From the Allerød to the mid-Holocene: palynological evidence from the south basin of the Caspian Sea☆

Suzanne A.G. Leroy [a,*], Alina Tudryn [b,c], Françoise Chalié [d], Lourdes López-Merino [a], Françoise Gasse [d]

[a] Institute for the Environment, Brunel University, Uxbridge, UB8 3PH London, UK
[b] Univ Paris-Sud, Laboratoire IDES, UMR8148, Orsay F-91405, France
[c] CNRS, Orsay F-91405, France
[d] CEREGE, UM 34 Aix-Marseille Université-CNRS UMR 7330- IRD UMR 161, Europôle Méditerranéen de l'Arbois, BP80, F-13545, Aix-en-Provence Cedex 04, France

ARTICLE INFO

Article history:
Received 18 June 2013
Accepted 31 July 2013
Available online 2 September 2013

Keywords:
Caspian Sea
Pollen
Dinocysts
Vegetation
Sea level fluctuations
Palaeohydrography
Younger Dryas
Holocene

ABSTRACT

Pollen and dinoflagellate cysts have been analysed in a core from the south basin of the Caspian Sea, providing a picture of respectively past vegetation and water salinity for the Late Pleistocene to middle Holocene. A relatively sharp lithological change at 0.86 m depth reflects a shift from detrital silts to carbonates-rich fine silts. From this depth upwards, a Holocene chronology is built based on ten radiocarbon dates on ostracod shells and bulk carbonates.

From the vegetation point of view, the Late Pleistocene deserts and steppes were partially replaced in the most sheltered areas by an open woodland with *Pinus, Juniperus-Hippophae-Elaeagnus* and even *Alnus-Quercus-Pterocarya* and *Fraxinus*, related to the Allerød palynozone. This was interrupted by the Younger Dryas palynozone when *Artemisia* reaches a maximum in a first instance followed by a very dry phase with only a slight return of *Pinus* and *Quercus* and the rare presence of *Ulmus-Zelkova*. From 11.5 to 8.4 cal. ka BP, an open landscape dominated by shrubs such as *Ephedra* and progressively increasing *Quercus* appeared. The final spread of diverse evergreen and deciduous trees is delayed and occurs after 8.4 cal. ka BP. It is suggested that this delay is caused by an arid climate in the Early Holocene linked to high insolation and perhaps to a lake effect.

The dinocyst assemblages fluctuate between slightly brackish (*Pyxidinopsis psilata* and *Spiniferites cruciformis*, 7 psu and lower) and more brackish (*Impagidinium caspienense*, ~13 psu). In the Lateglacial (Khvalynian highstand), the assemblages remained dominated by relative low salinity taxa. A late and brief increase of salinity occurred prior to 11.2 cal. ka BP associated with the Mangyshlak lowstand. It is suggested that it was caused by a brief drop in meltwater flow from both the north and the southeast (Uzboy) and a likely evaporation increase. This lowstand occurs quasi at the same time as the end of a longer lowstand in the Black Sea. The freshest waters are then inferred as having occurred between 8.4 and ≤4.4 cal. ka BP, linked to a connection with the Amu Darya and the melting glaciers on the Pamir Mountains.

The Caspian Sea is a sensitive environment, easily perturbed by global climatic changes, such as the Allerød and Holocene warming, and the Lateglacial and Younger Dryas cooling, as well as by regional changes in its hydrography, such as shifts in the Eurasian meltwater and the Volga and Amu Darya inflows.

1. Introduction

The levels of the Caspian Sea (CS, 36–47 °N, 47–54 °E), the world's largest lake (Fig. 1A and B), have changed dramatically over various timescales (Kazancı et al., 2004), causing deep modifications in both the volume and area of this large water body, larger than the British Isles. During the 20th century, CS water levels have fluctuated rapidly, a hundred times faster than recent global sea level,

* Corresponding author. Tel.: +44 1895 266087; fax: +44 1895 269761.
E-mail address: suzanne.leroy@brunel.ac.uk (S.A.G. Leroy).

0277-3791/$ – see front matter © 2013 The Authors. Published by Elsevier Ltd. All rights reserved.
http://dx.doi.org/10.1016/j.quascirev.2013.07.032

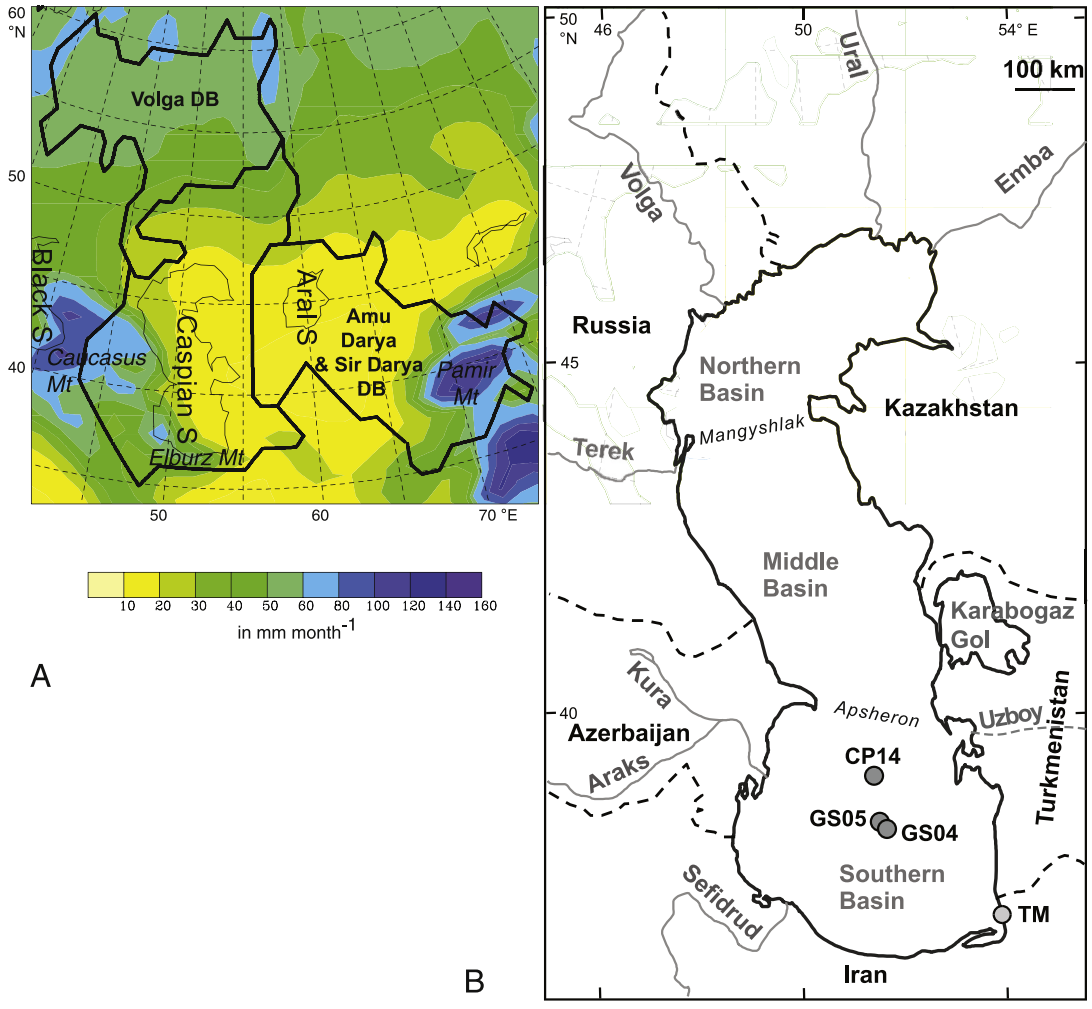

Fig. 1. A: Mean annual precipitation for the area of the Caspian and Aral Sea drainage basins (data from the ECMWF interim reanalysis). Colours indicate different mm per month values. Black lines: drainage basin limits with to the North the Volga catchment and to the East the Aral one. DB: drainage basin. S: sea. Mt: mountain. 1B: Location map of the cores and the main inflows to the Caspian Sea. Black dashes lines are borders. Grey lines are rivers, continuous line for permanent, dashed line for temporary. Grey circles for core locations. (For interpretation of the references to colour in this figure legend, the reader is referred to the web version of this article.)

causing serious environmental and economic damage and adversely affecting oil and gas exploitation, agriculture and fishing as well as causing major risks in areas for storage of nuclear waste. Instrumental records (since 1837) indicate a 3 m change with a sharp drop between 1930 (−26 m) and 1977 (−29 m), followed by a sharp rise until 1995 (−26.5 m) (Leroy et al., 2006; USDA, 2013). The precise causes of these changes are not well understood: they are believed to result from a combination of climate, human impact and tectonic activity (e.g. Shiklomanov et al., 1995; Froehlich et al., 1999).

The impact of water level changes was especially strong in low-lying areas. The horizontal changes were the most pronounced in the north basin with the Volga delta wandering north–south up to 700 km along its riverbed in the last climate cycle (Kroonenberg et al., 1997; Tudryn et al., 2013) (Fig. 1B). A vertical amplitude of c. 150 m has been reconstructed for the Last Glacial period and Early Holocene between a glacial highstand of +50 m (the Early Khvalynian highstand, perhaps at 17–15 ^{14}C ka BP or much earlier) and an Early Holocene lowstand (the Mangyshlak lowstand, c. 9 ^{14}C ka BP) of possibly lower than −110 m (Rychagov, 1997; Chepalyga, 2007). Poorly known past low levels are mostly defined by bathymetry and seismic surveys (such as palaeo-canyons and underwater terraces), besides the onshore sedimentation hiati.

The palaeoenvironmental history around the CS is poorly known due to the scarcity of long-sequence studies in the area. The way in which the climate has changed in the region around the CS, the extent to which climate may have influenced the water level itself, and whether any lake effects influenced climate are not well understood, or even not yet investigated. The same is true for vegetation, as it is not known how climate could have affected landscape change in this very biodiverse area from subtropical vegetation to the south and desertic one to the north and east (Leroy et al., 2007). The short regression to glacial conditions and its environmental consequences, at the transition between the glacial and interglacial periods, i.e. Younger Dryas (YD) stadial (12.8–11.5 cal ka BP; Muscheler et al., 2008), have not yet been identified in the region.

A palynological approach could give information on both water level/salinity changes and vegetal landscape. Dinoflagellate cysts (dinocyst) are widely used to reconstruct salinities worldwide (Marret and Zonneveld, 2003). Dinocyst assemblages, cyst morphology and endemism may provide information about the impact of various environmental parameters and are a basis for palaeoenvironmental reconstructions (e.g. Mertens et al., 2009). The dinoflagellate cyst taxonomy of the CS has remained totally unknown until recently when many forms, species and even one

genus were described (Marret et al., 2004). Since this has been done, it has become possible to investigate them in sedimentary sequences: e.g. 1) Pliocene oil and gas reservoirs in Azerbaijan (Vincent et al., 2010), 2) the Holocene (with a hiatus in the reconstructed lowstand at 7.2–3.5 cal. ka BP) in the TM core taken in the southeastern corner of the CS (Leroy et al., 2013a), 3) the last 5500 years in short cores from the deep south and middle basins (Leroy et al., 2007), 4) the last hundred years in coastal lagoons of northern Iran (Leroy et al., 2011) and 5) the last decades in the KaraBogaz Gol (Leroy et al., 2006). Owing to these studies, it has been possible to reconstruct the palaeosalinity of the CS and determine that it has fluctuated between more brackish (c. 13 psu) and closer to freshwater (c. 3–7 psu) (Leroy et al., 2007) in the last 10,000 years. Regarding vegetation change, pollen studies have highlighted the biogeographical importance of the area as a refuge of Arcto-Tertiary thermophilous species now extinct in Europe and the role of human impact on landscape change (Djamali et al., 2011, 2012).

The present work investigates a deep-sea sediment sequence of the south basin of the CS, core GS05 (Fig. 1B), where sediment formed even during lowstands. It combines dinocyst assemblages (past salinities), pollen and spores (terrestrial vegetation) and non-pollen palynomorphs (NPP) during the Late Pleistocene and the first half of the Holocene, in order to reconstruct terrestrial vegetation, biodiversity changes, sea levels and climate.

2. Study area

2.1. Geographical setting, climate and vegetation

The relief around the CS is roughly of two types: low lying in the northern half and the east side and high mountains in the southwest corner (the Caucasus Mountains) and the south (the Elburz Mountains).

Because of its great meridional extension, the CS straddles several climatic zones. The northern part of the drainage basin lies in a zone of temperate continental climate with the Volga catchment well into the humid mid-latitudes. The west coast features a moderately warm climate, while the southwestern and the southern regions fall into a subtropical humid climatic zone. The east coast has a desert climate.

Vegetation around the CS consists in the east of a northward gradient from desert (Chenopodiaceae and *Artemisia*) to steppe (*Artemisia* and several species of Poaceae): Irano-Turanian in the southeast (summer rainfall and cold winters) and Kazakho-Dsungarian in the west, north and northeast (winter rainfall) (Walter and Breckle, 1989). These authors mention freshwater holes in the desert between the Aral Sea and the CS with local vegetation made of *Populus*, *Elaeagnus*, *Salix* and *Alnus*, as well as *Calligonum* and *Tamarix*. A very diverse vegetation including vast mesic and altitudinal forests, i.e. the Hyrcanian forest, has developed in the two mountain ranges (Walter and Breckle, 1989), even including refugial areas for some past European species such as *Parrotia persica* (Leroy and Roiron, 1996). Today the biogeographical distribution of *P. persica* is reduced to the coastal area south of the CS and to the Caucasus up to 1500 m altitude, where the tree lives in a mild and humid climate all the year round (Leroy and Roiron, 1996).

2.2. Hydrological and biological setting

The CS is the world's largest lake in terms of both area and volume (Fig. 1A and B). The altitude of the surface was at 27 m bsl in 1994, at the time of the coring. Three basins divide the sea, deeper from the north to the south: the northern basin (80,000 km^2) with an average depth of 5–6 m and a maximum depth of 15–20 m; the middle basin (138,000 km^2) with an average depth of 175 m and a maximum depth of 788 m; and the southern basin (168,000 km^2) with an average depth of 190 m and a maximum depth of 1025 m (Fig. 1B). The southern basin holds more than 65% of the Caspian water volume. The Mangyshlak threshold separates the north and the middle basins, while the Apsheron sill divides the middle basin from the south one (~180 m water depth).

The CS drainage basin covers about 3.1 million km^2, stretching from 35 to 62°N (Fig. 1A). Water inputs comprise river discharges, in particular the Volga (contributing 80–85% of the total), Kura, Ural and Terek Rivers (Rodionov, 1994). Then a series of smaller rivers bring water from the west and south sides of the CS, while the eastern side has nowadays hardly any river because of the dry climate and the large expanses of desert and steppe.

This pattern of river inflow induces a North–South positive gradient of water salinity. It increases from freshwater in the northern end of the basin to an almost homogeneous 12.5–13.5 practical salinity unit (psu) in the middle and southern basins. In the southern basin, seasonal salinity changes are less than ~0.2–0.4 psu. The mean annual salinity increases from the surface to the bottom waters from 0.1 to 0.3 psu (Zenkevitch, 1963; Kosarev and Yablonskaya, 1994; Rekacewicz, 2007a). The mean sea surface temperature in winter ranges from zero in the north to 10 °C in the south, and in summer from 21 in the east to 28 °C in the south (Rekacewicz, 2007b). A deep water mixing occurs twice a year (Dumont, 1998).

Climatic change has an influence on sea levels via not only evaporation and precipitation over the sea but also on the drainage basin, especially of the Volga River (Arpe et al., 2013). From a meteorological point of view, CS levels are influenced by precipitation over the Volga drainage that has a peak discharge in May (Arpe et al., 2000, 2012, 2013). Over the 20th century, a connection between CS level and ENSO has been highlighted, but not with NAO (Arpe et al., 2000; Arpe and Leroy, 2007). During glacial periods, this simple relationship is complicated by large influx of meltwater and climatic feedbacks. Over the deglaciation period, in addition to climatic changes the palaeohydrology around the sea has caused many changes to the CS water budget. After the Last Glacial Maximum (LGM), it has been suggested that the melting of the Eurasian ice cap and the re-routing of north flowing rivers to the south have accelerated a water transfer from the north (via River Volga and via Aral Sea/Uzboy pass) to the CS and then to the Black Sea (Chepalyga, 2007). The Uzboy River reached the CS 100 km south of the KBG in the Krasnovodsk Bay in the Late Pleistocene and episodically in the Holocene but few details only are known (Létolle, 2000). This river brought a considerable supply of freshwater to the south basin. The lower section of the Uzboy River (Fig. 1B) received water from the Aral Sea and the Amu Darya through the Sarykamysh River, which are fed by the Pamirs and part of the Hindu Kush (Boomer et al., 2000; Sorrel et al., 2006; Austin et al., 2007). The Amu Darya seemed to have been flowing intermittently in the CS until as recently as in the 14–16th century AD, not only for climatic reasons but also due to man-made river avulsions (Létolle, 2000; Naderi Beni et al., 2013).

Owing to its isolation, the CS has a high level of endemism (e.g. Dumont, 1998). The biodiversity results from a combination of various origins: Atlantic-Mediterranean connection (because of the Paratethys link), Arctic Sea connection (because of the rivers flowing from the north to the south during glacial meltwater phases, via the Aral Sea) and river connections (Grigorovich et al., 2003; Marret et al., 2004). Past history of the CS, resulting in the alternation of brackish and fresher water periods, has had a strong impact on the present-day biodiversity.

The CS biota ranges from freshwater to brackish to euryhaline with species of freshwater origin tolerating salinities up to 13 psu and species of marine origin tolerant to salinities down to 13 psu (Dumont, 1998). Dinoflagellates are one of the most abundant phytoplankton groups, second to the diatoms. In the CS, phytoplankton richness is rather low, in comparison with other open seas, with a dominance of fresh and brackish water species in the North Basin and a higher occurrence of marine (euryhaline) and brackish species in the middle and southern basins (Kosarev and Yablonskaya, 1994). Surveys in the 1960s and 1970s showed that dinoflagellates composed only 9% of the phytoplankton population, whereas a recent survey in 2001 shows that dinoflagellates consist of almost half of the population (Kideys et al., 2005).

2.3. Sea-level fluctuations and their possible causes

The continuously fluctuating levels of the CS change both erratically and cyclically (Kazancı et al., 2004). It is nevertheless generally accepted that transgressions are accompanied by freshening of water masses and cold climate and that regressions correspond to an increased salinities and warm climate (Ferronsky et al., 1999; Ryan et al., 2003), having a reverse behaviour to that of the global ocean. Ferronsky et al. (1999) are of the firm opinion that transgressions and regressions are driven mostly by climatic change. They propose as evidence that transgressions have always been preceded by "climate cooling and wetting".

It has also been suggested that forests develop during the transgressive phases, while arid vegetation dominates in the regressive phase (Kuprin and Rybakova, 2003). An attempt at describing the main transgressions and regressions since the end of the Pleistocene was made, but the ages and even the number of regressions and transgressions are still very much a question of debate. Notably what is happening at the crucial time of the Pleistocene–Holocene transition is far from clear.

At the end of the Pleistocene, large ice-dammed freshwater lakes formed along the southern edge of the ice sheet, such as palaeolakes Mansi and Komi (Grosswald, 1993; Mangerud et al., 2001). The history of these palaeolakes' drainage is poorly documented but the withdrawal of their meltwater inflow must have governed the change of the CS from a freshwater lake to a more saline water body. The last Late Pleistocene transgression, the **Khvalynian highstand**, is characterised by a large freshwater lake whose age is not precisely known (Rychagov, 1997). According to Chepalyga (2007) it began at c. 16 ^{14}C ka BP and ended with the Mangyshlak lowstand at 10 ^{14}C ka BP. The water origin is multiple, such as rivers (both the Amu Darya with water from the Pamirs and N–S rivers that could not flow to the north, being blocked by the Eurasian ice cap), and meltwater from both the ice cap and permafrost (Forte and Cowgill, 2013). Some scientists suggest, however, a strictly climatic origin of the highstand with an increase of precipitation on the Volga basin (Sidorchuk et al., 2009). Other authors, when comparing sedimentation rates in cores from the south basin to the middle basin, find a much higher sedimentation rate in the south and also much fresher waters (Ferronsky et al., 1999). They are led to suggest river inflow from the East by the ancient Amu Darya and they support their hypothesis by the oxygen isotope results that allow excluding a major influence of the Volga in the south basin at that time. However their results were obtained from oxygen isotopes on bulk sediment and may have been affected by detritic carbonates. Another perhaps stronger argument comes from the Apsheron sill that shows for that period an entrenchment with the evidence of a south-to-north water flow (Ferronsky et al., 1999; Kuprin et al., 2003). The best indirect dates for the highest water levels within the Khvalynian period come from the Black Sea: a series of successive massive meltwater pulses

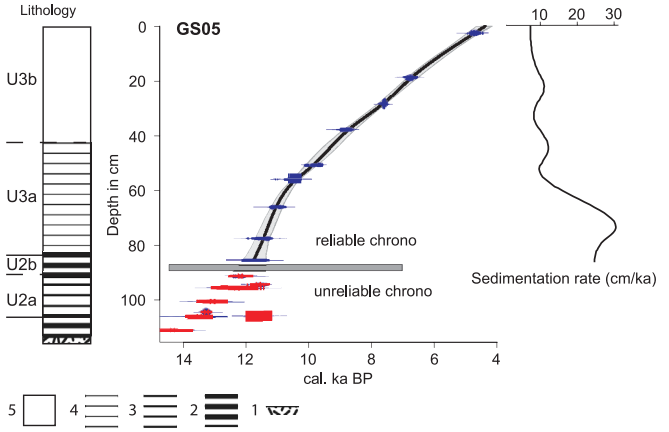

Fig. 2. Age–depth model and sedimentation rate for the upper 86 cm of GS05 core. Radiocarbon dates are in blue for the interval with reliable chronology, while they are in red for the unreliable one. 1: oblique lamination, 2: coarse lamination with dark layers, 3: fine lamination, 4: pale lamination, and 5: absence of lamination. (For interpretation of the references to colour in this figure legend, the reader is referred to the web version of this article.)

from the CS via the Manych–Kerch connection have been recognised in the Black Sea between 18 and 15.5 ^{14}C ka BP (Bahr et al., 2005). The **Younger Dryas stadial** is generally considered as a period of transgression both in the Black Sea (Ryan et al., 2003) and in the CS (Chalié et al., 1997).

The **Mangyshlak lowstand**, like most regressions, is less well known than the Khvalynian highstand. It is usually considered to have taken place between 10 and 8.5 ^{14}C ka BP with a decrease of the level as far down as possibly 110 m bsl or even more (Mayev, 2010). The Mangyshlak lowstand has mostly been identified by hiatus in outcrops and the geomorphology of the seabed. Sedimentary sequences containing sediment of this lowstand have been found in the three basins of the CS, which is often characterised by slightly coarser sediment and a lower carbonate content than in the subsequent Neocaspian (also known as Novocaspian) period (Mayev, 2010). The latter author has suggested a step-wise decrease of the water level to a minimum at 9 ^{14}C ka BP, followed by a sharp re-increase estimated at 20 cm per year. It has been proposed that the sediment is more influenced by rivers, with a clear contribution from the east probably from the Uzboy River (Mayev, 2010). The lowstand is caused by the decrease of meltwater availability and by a dry climate. It is during this dry period that the loess on the Iranian coast may have formed (Kazancı et al., 2004) and the Amu Darya switched its flow from the south basin to the Aral Sea (Boomer et al., 2000). A revision by Svitoch (2012) suggests that the first regression of the Holocene should be called the Enotaev lowstand and that the Mangyshlak is a younger regression. In order to keep with the most frequently used stratigraphical schemes, we will follow Mayev (2010) and Sorokin (2011)'s usage and consider that the regression at the beginning of the Holocene is the Mangyshlak. However we take into account that other lowstands maybe have existed after the Mangyshlak one.

During the Holocene, the reconstructed levels are generally intermediate (**Neocaspian transgression**) with some fluctuations, but their amplitude, number and timing diverge deeply between authors (Mamedov, 1997; Rychagov, 1997; Kakroodi et al., 2012; Svitoch, 2012).

2.4. Previous studies on core GS05

Several publications have already come out on the sedimentology of Late Pleistocene–Early Holocene core GS05, the object of

the present investigation. The results are briefly summarised here. Various lithological boundaries of this rather homogeneous sequence have been published, some based on visual descriptions (Chalié et al., 1997; Escudié et al., 1998; Jelinowska et al., 1998) and some based on geochemistry (Pierret et al., 2012). Here we have followed the visual one as it is the most common one (Figs. 2 and 3).

Unit 1 (986–111 cm) is a detrital-rich deposit, with a very regular alternation (every c. 8 mm) of brownish grey and dark layers that disappear through oxidation. The amount of carbonate is relatively low (21–25%) and the sediment is quasi devoid of authigenic biological remains. Oblique laminations from 121 to 118 cm suggest minor slumping.

Unit 2a (111–94 cm) consists of pale silts more finely laminated than below; while in **unit 2b** (94–86 cm) dark layers reappear.

After a sharp change, **unit 3** (86 cm-top) is a pale, dark beige calcareous mud (49–63%), vaguely laminated up to 44 cm depth (**unit 3a**). In **unit 3b** (>44 cm), the amount of carbonate slightly decreases and the sediment is more homogeneous. Diatoms appear progressively in the sediment from 80 cm onwards. Below this depth they are almost totally absent due to dissolution problems and/or low productivity.

Laminated silty sediment, from the lower units 1 and 2, is characterized by high and varying magnetic susceptibility values (between 150 and 300 10^{-5} S.I.), which reflect high contents of authigenic iron sulphide – greigite (Fe_3S_4) (Fig. 3). The presence of greigite indicates poorly oxygenated conditions at the bottom of the basin (Jelinowska et al., 1998, 1999). Varying contents of greigite explain the scatter in magnetic susceptibility. The calcareous mud from unit 3 is characterized by its low and rather homogeneous (between 50 and 60 10^{-5} S.I.) magnetic susceptibility (Fig. 3), which is due to low contents of detrital magnetite (Jelinowska et al., 1998). Preserved detrital magnetite indicates better oxygenated bottom conditions.

The magnetic mineralogy was attributed to the changes of the CS level (Jelinowska et al., 1998; Bol'shakov et al., 2009), with authigenesis of greigite in poorly ventilated basin and less saline bottom waters during highstands, and detrital magnetite in better ventilated and more saline waters during lowstands. In this way, the change of the magnetic mineralogy between units 2 and 3, could be related to the major decrease of the CS level (end of the Khvalynian highstand), due to a lowering of the water supply from the catchment area.

A synthetic pollen curve for the whole core, **GS05**, was presented in Pierret et al. (2012) with emphasis on the vegetation cover extend and the weathering process. The chronology was based on corrected dates that were not calibrated.

2.5. Previous studies in the area

Some palynological analyses have been published from a deep-sea core taken in almost the same coring station covering from the Khvalynian highstand to the older part of the Neocaspian period:

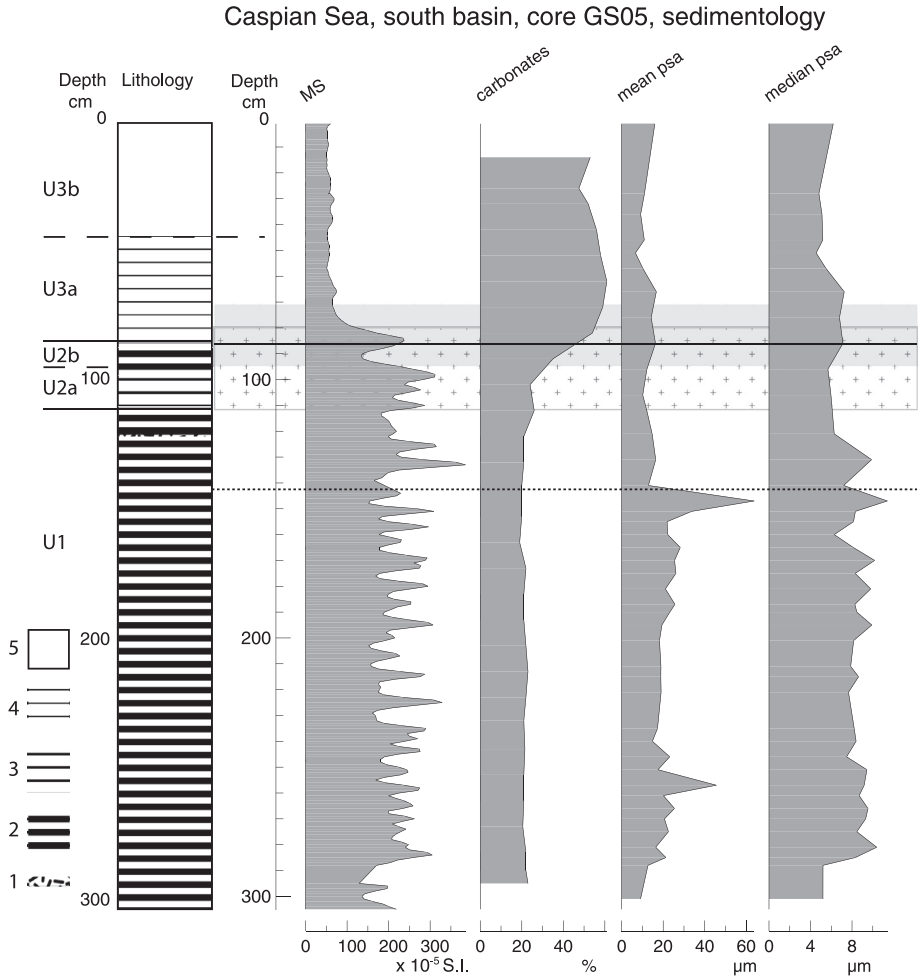

Fig. 3. Sedimentological data: lithology, magnetic susceptibility (MS), carbonate content (after Chalié et al., 1997) and particle size analysis (psa) of core GS05. Lithological symbols as in Fig. 2. The horizontal dashed line shows the drop of particle size. The horizontal box with crosses highlights the Younger Dryas stadial, and the light grey one the Mangyshlak lowstand. Thin horizontal black line across the figure shows where a reliable chronology starts.

core GS04 (Kuprin and Rybakova, 2003) (Fig. 1B). The Khvalynian–Neocaspian transition has been recognised at 105 cm depth, a few cm below a radiocarbon age of 9.1 ^{14}C ka BP at 80 cm on bulk sediment not corrected for the detrital fraction (Ferronsky et al., 1999), and is characterised by a clear increase of authigenic carbonates. Broadly the same changes of the magnetic susceptibility were recorded in core GS04 than in core GS05 (Kuprin et al., 2002, 2003). Late Khvalynian sediments are characterised by high magnetic susceptibility values due to the presence of iron sulphides; while in the Neocaspian, low values of the magnetic susceptibility are correlated with the decreased contents of iron sulphides (Kuprin et al., 2002, 2003). The pollen and spores samples were poor and contained a significant amount of reworked elements; only a table with some occurrences (low counts, <50 pollen and spores, no dinocysts) has been published; but it is difficult to interpret and use here (Kuprin and Rybakova, 2003). Diatoms were more abundant (Kuprin and Pirumova, 2002) and show a clear salinity change from freshwater in the Khvalynian highstand (rare occurrences of diatoms) to more saline in the Neocaspian period (abundant diatoms). Neither the Mangyshlak lowstand nor internal fluctuations to the Neocaspian were recognised (Kuprin et al., 2003).

The pollen and dinocysts interpretation for **three cores** covering the second part of the **Holocene** taken during the same cruise as cores GS04 and GS05 were published in Leroy et al. (2007). The main results are the alternation of two palynomorph assemblages over the period 5.5 to 0.8 cal. ka BP: two slightly less brackish (salinities <7 psu) phases with pollen transported by river, interrupting longer periods of slightly more brackish phases (similar to the present) with wind-transported pollen. The end of a long less brackish phase, attributed to the Gousan highstand (sensu Svitoch, 2009) (or perhaps the Late Khvalynian highstand), is at 3.9 cal. ka BP in core CP14, and it is followed by a shorter one from 2.1 to 1.7 cal. ka BP, attributed to one of the highstands in the Neocaspian period.

Pollen and dinocyst diagrams were published for a core taken in the **SE corner** of the CS, which covers most of the Holocene but with a significant hiatus in the middle from 7.2 to 3.5 cal. ka BP (Leroy et al., 2013a). The results indicate a clear vegetation succession out of the glacial refugia in the Elburz Mountains, the Mangyshlak lowstand at the beginning of the Holocene, a highstand from 10.6 to 7.2 cal. ka BP, a lowstand from 7.2 to 3.5 cal. ka BP with a minimum at 3.9 cal. ka BP, and then intermediate water levels onwards.

3. Material and methods

3.1. Coring

Cores were taken in the south basin during a French–Russian oceanographic cruise in August 1994, on-board a Russian military ship rented for the expedition. All the locations were chosen to avoid direct river delta influence, and other disturbances as far as was known at the time. Large-scale slope failure processes are described by Richardson et al. (2011) using seismic with an average vertical resolution (quarter of the wavelength) of 20 m on the north-west slope of the basin that is much steeper than the east side where coring was located. Due to bad weather, it was however impossible to obtain reliable seismic profiles, water depths and geographical coordinates. Two coring techniques were combined with the aim of recovering complete sections from the Late Pleistocene and the Holocene. The Kullenberg cores, typically 10 m long, 90 mm of diameter, have probably lost c. 1–1.5 m of sediment at the moment of penetration by the corer barrel. The Pilot cores, associated to the Kullenberg cores, c. 150–200 cm long, have also lost a few decimetres for the same reason. Half the cores are kept in a repository at the geology laboratory of the Museum National d'Histoire Naturelle (Paris, France) and the other half at the Moscow State University, Russia. The French cores were sliced into two parts, one kept as an archive and the second used for sampling. The depths are provided in composite depth due to the existence of two small gaps in the top metre section.

Table 1
Names and location of some of the cores in the south basin of the Caspian Sea taken during the French–Russian expedition of 1994, presented or discussed here, and of a core from the S-E Caspian Sea, Iranian coast (see Fig. 1B for location on the map and text for explanations).

Here	On board no	Museum no Core length (cm)	Station	Latitude (N), longitude (E), Water depth (m)
GS05	SR9402GS05	SR01GS9405 957	2	38°45′39″, 51°32′16″ 518
CP14	SR9406CP16	SR01GS9414CP 140	6	39°16′, 51°28′ 330
GS04	SR9402 GS04	n/a 787	2	38°41′39″, 51°36′36″ 405

Core name	Core length (cm)	Altitude	Latitude (N), longitude (E)
TM	2750 cm	2 m above sea level, i.e. −25.5 m	37°09′06″, 54°03′24″

The results of a study of the top 305 cm of the 10 m-long GS05 core are presented here (Table 1). The bottom part of the core was not investigated in detail because it presents identical ages either due to problems with radiocarbon dating, or due to an extremely rapid deposition of the sediment.

3.2. Lithology

The particle size analysis is a new proxy for this sequence. It was obtained by laser granulometry on bulk sediments using a Coulter LS 130 apparatus. Fifty samples were analysed for the top 305 cm of the core.

3.3. Radiocarbon dating and corrections

Establishing a chronological framework for sequence GS05 proved to be a complex task, as adequate material for radiocarbon dating is rare. Organic matter, bulk carbonates and ostracod valves are discussed.

3.3.1. Organic matter

Total organic content (TOC) is very low through the whole sediment sequence GS05. TOC, measured each 10–20 cm (Chalié et al., 1997), showed values lower than 1%. Organic macroremains, appropriate for radiocarbon analyses, were not found.

3.3.2. Bulk carbonates

Calcimetry measurements of bulk sediment show that carbonates occur along the whole sequence (Fig. 2). Mineralogical analysis, as detailed by X-ray diffraction analyses, indicated that different carbonate types are present in the sediment (Chalié et al., 1997). Based on the calcite crystallinity index (which is given by the XRD (104) peak width at mid height), the Mg-content of the high-Mg calcite, and microscopic observations, enabled us to distinguish three types. First fine, isodimensional (few μm), spindle-shaped Mg-calcite crystals, were identified as a major component of the sediment above 86 cm depth, and present above 111 cm depth (Chalié et al., 1997). These carbonates were observed in the surficial

sediments in the southern CS basin, and were shown to precipitate in surface waters, during the warm season (Escudié et al., 1998): they were therefore considered as the authigenic fraction of the total carbonates in the sediment. Secondly very rare carbonated biological remains were also identified (such as coccoliths and ostracods). Finally, a well-crystallised, Mg-poor calcite fraction of eroded rounded calcite grains was considered as detrital in origin. XRD–inferred mineralogical characters of the sediment therefore enabled us to determine the relative proportions of authigenic *versus* detritic carbonates, for the upper 86 cm. Below this depth, carbonates are less abundant, the detritic fraction dominates, the authigenic carbonates are almost absent from the sediment, implying reduced validity of corrections on radiocarbon dates. Moreover, the two carbonate fractions – authigenic and detritic – become difficult to infer from XRD analysis, since Mg-content of authigenic carbonates decreases with sediment depth. The ratio between authigenic and detritic carbonates allows correcting the radiocarbon activity obtained from bulk sediment (Table 2).

Several corrections must be applied to raw values of radiocarbon dates on bulk carbonate material, to account for (1) the ageing of modern surface waters (in which the authigenic carbonates precipitates), which shows that the equilibrium between modern surface waters and atmospheric CO_2 is not complete, and (2) the amount of detrital carbonates.

Total Dissolved Inorganic Carbon (TDIC) was measured for several water depth profiles, and water was sampled during the sea expedition of years 1994 and 1995 (Escudié et al., 1998). Surface waters reveal a present-day ^{14}C activity value of ~109 pMC (percent Modern Carbon). At the sea bottom, the TDIC ^{14}C activity decreases to ~95–96% in the southern basin. The present-day atmospheric CO_2 is estimated at about 117% at the latitude of the CS (Levin et al., 1995). The 8% difference in ^{14}C activity between modern surface water TDIC and atmospheric CO_2 demonstrates that equilibrium between surface waters and atmosphere is not reached. We assumed that this disequilibrium was constant through time. We therefore calculated the radiocarbon ages from ^{14}C activities, using 92% for the water TDIC, instead of the 100% reference value for atmospheric CO_2, before the bomb effect of nuclear weapon testings (Table 2).

Following the procedure described in Fontes et al. (1993), the radiocarbon ages were corrected from the detrital fraction. The procedure is appropriate for the upper 86 cm depth; it is not applicable at all below 111 cm depth, as it was not possible to differentiate authigenic from detrital carbonates. For samples between 111 and 86 cm depth, the ages obtained after corrections of detrital carbonates show very large errors, and should be treated with caution.

The correction of apparent radiocarbon measured ^{14}C activity, for bias due to the detrital carbonates, is based on the mass balance principle applied to the radiocarbon activities, and making the reasonable assumption that detritic calcite is old enough to contain dead carbon only (Fontes et al., 1993).

3.3.3. Ostracod shells

Ostracod shells, considered as authigenic carbonates, were hand-picked under a binocular laboratory stereo-microscope. Shapes of the shells indicate a state of good preservation. XRD analysis confirmed that the carbonated shells were not re-

Table 2
Radiocarbon chronology of sequence GS05 (see text for explanation of the different carbonates types, and for corrections applied to the radiocarbon dates). Radiocarbon ages were calibrated using the IntCal09.14C calibration (Reimer et al., 2009).

Mean depth (cm bsl)	Depth interval (cm)	N° sample (Orsay, Gif s/ Yvette)	Dated material	^{14}C age (yr BP)	± (yr BP)	Age corrected from detrital $CaCO_3$ and surface waters ageing	$CaCO_3$ authigenic fraction (%)	Two σ ranges (cal yr BP)	Relative area under distribution (%)
2.50	2–3	H994	Bulk carbonates	5400	80	4194	94.56	4446–4471	0.01
								4516–4877	0.98
								4942–4951	0.01
18.50	18–19	H1596	Bulk carbonates	7281	90	5927	92.85	6500–6520	0.01
								6530–6980	0.99
28.50	28–29	H1597	Bulk carbonates	8252	80	6759	91.26	7470–7760	0.99
								7780–7780	0.01
35.75	35.5–36	H1527	Bulk carbonates (<10 μm)	9106	100	7983	95.56	8586–9094	0.99
								9098–9123	0.01
50.50	50–51	H1083	Bulk carbonates	9930	90	8721	94.54	9530–9950	0.91
								9990–10,010	0.01
								10,020–10,040	0.01
								10,060–10,140	0.06
								10,140–10,150	0.01
55.50	53.5–57.5	GifA 98,109	Ostracod shells	9610	100	9240		10,220–10,700	1
56.00	55.5–56.5	H1293	Bulk carbonates	10,533	120	9293	94.18	10,221–10,787	0.99
								11,033–11,061	0.01
66.00	65.5–66.5	H1294	Bulk carbonates	10,968	110	9678	93.59	10,700–11,260	1
75.50	75–76	H1299	Bulk carbonates	11,181	120	9917	93.89	11,130–11,830	0.97
								11,870–11,960	0.03
85.50	85–86	H1300	Bulk carbonates	11,674	140	10,089	90.21	11,225–12,145	1
91.25	91–91.5	H1465	Bulk carbonates	12,993	110	10,336	78.94	11,760–12,540	1
94.25	92–92.5	H1486	Bulk carbonates	15,484	80	10,007	55.57	11,240–11,820	0.99
								11,940–11,950	0.01
95.50	95–96	H1301	Bulk carbonates	18,841	290	10,596	39.37	11,408–11,440	0.01
								11,475–11,555	0.01
								11,598–13,103	0.98
100.50	100–101	H1319	Bulk carbonates	19,254	260	11,186	40.25	12,588–13,519	0.99
								13,528–13,574	0.01
104.25	104–104.5	H1487	Bulk carbonates	18,143	90	11,416	47.56	13,110–13,440	1
105.75	104–107.5	GifA 99,071	Ostracod shells	10,310	130	9940		11,160–11,980	1
106.00	105.5–106.5	H1308	Bulk carbonates	16,050	220	11,595	63.11	12,983–13,006	0.01
								13,069–13,935	0.99
111.00	110.5–111.5	H1318	Bulk carbonates	16,577	190	12,182	63.59	13,674–14,988	1

crystallised, and hence were a relevant material for dating. Identified species were benthic.

The apparent measured activities must be corrected for two biases (Table 2). First, the disequilibrium between TDIC and atmospheric CO_2, observed on the present-day system, were corrected with the same procedure as for bulk carbonates. Secondly, residence time was determined by the difference of radiocarbon activity between modern surface and bottom waters (Escudié et al., 1998), and was estimated at about 370 years. This was used to correct ages obtained on benthic ostracod shells that precipitate in sea bottom waters. The 370 years reservoir correction is consistent with the mean value of 410 years, obtained in the northern basin of the CS (Kuzmin et al., 2007).

3.3.4. Calibration and age–depth model

After corrections, radiocarbon ages were calibrated using the IntCal09.14C calibration curve (Reimer et al., 2009) and an age–depth model for the dates above 86 cm was obtained using Clam.R 2.1 (Blaauw, 2010). A good fit was provided by a smooth spline solution with a smooth factor of 0.3.

3.4. Palynological methods

The processing of 57 samples (on average 1.2 ml) involved the initial addition of sodium pyrophosphate to deflocculate the sediment. Samples were then treated with cold hydrochloric acid (10%) and cold hydrofluoric acid (32%), followed by a repeat HCl. The residual fraction was then screened through 120 and 10 μm mesh sieves and mounted on slides in glycerol and sealed with varnish. *Lycopodium* tablets were added at the beginning of the process for concentration estimates, given as number of microfossil per ml of wet sediment.

The number of pollen grains counted (excluding spores and NPP) is at minimum 231, and on average 324. Dinocysts were counted at the same time as the other microfossils. The sum for percentages is made of all dinocysts, and its minimum is 109, with an average of 335 cysts. A pollen concentration on dinocyst concentration ratio (*P*/*D*) was determined according to McCarthy and Mudie (1998) to estimate the degree of continentality of the assemblages.

Diagrams were plotted using Psimpoll (Bennett, 2003) with 10× exaggeration curves and black dots for values lower than 0.5%.

Pollen and spores were identified using the atlas of Reille (1992, 1995, 1998) and the Brunel pollen reference collection. Dinocysts and some NPP were identified following illustrations in Marret et al. (2004), Sorrel et al. (2006), Leroy (2010) and Mudie et al. (2011).

3.5. Numerical methods

Zonation was calculated separately for pollen and spores, and dinocysts by cluster analysis (CONISS) after square root transformation. Principal Component Analysis (PCA) was also applied separately for pollen and dinocyst datasets. PCA exploration was performed using SPSS 15.0, in correlation mode and applying varimax solutions. Data were square-root transformed prior to analysis. For pollen data, hydro-hygrophytes and NPP were excluded. For trees, shrubs and herbs, only taxa with percentages higher than 1% in at least one sample were considered. The sums of trees and shrubs were also incorporated. All dinocyst taxa have been included, and in this PCA of dinocyst data, data from the nearby core CP14 (Leroy et al., 2007) have also been included in an attempt to identify what the possible overlap is between the two cores.

In order to detect diversity changes in core GS05, palynological richness was estimated by rarefaction analysis on terrestrial pollen types, using the open software PAST 2.17c (Hammer et al., 2001). The lowest sum was used as standardized count, being 231.

4. Results and interpretation

4.1. Age–depth model

The results of radiocarbon dates, corrections of biases, transfer into calendar timescale and age–depth modelling are reported in Table 2 and Fig. 2. Due to the combination of low carbonate contents, associated with high detrital carbonates, low authigenic fraction and the error on the measurement of the proportion of authigenic fraction, radiocarbon dates are highly speculative below 86 cm depth: the cumulative errors on the measurements present very high values. Corrections being still possible for dates between 111 and 86 cm depth, these were shown in a tentative chronological framework. But below 86 cm depth, older than 11.8 cal. ka BP, corrected radiocarbon dates show no trend and indicate a uniformity of the ages. The period is a crucial one for radiocarbon dating, as it includes a large ^{14}C age plateau. Finally, dates in the interval 111–86 cm on ostracod shells and on bulk carbonates at the same level (~106 cm depth) showed quite different results (Table 2).

To the contrary, the validity of the corrected ages above 86 cm depth is reinforced by their chronological sequence of all the dates and by the consistency between an age obtained on bulk carbonates and one on ostracod shells at almost the same level, 56 and 55.5 cm depth (Table 2).

4.2. Lithology

Our sequence shows, on the whole, little changes and mean grain sizes corresponding to the fine silts. In most of unit 1, the grain size varies between 10 and 25 μm, but with some higher values that indicate the presence of a sandy fraction at 260 and 245 cm (Fig. 3). Above 142 cm (last part of unit 1 and units 2 and 3), mean grain sizes are lower and less scattered.

In the nearby core GS04, Kuprin et al. (2003) obtained broadly similar values, varying between ~17 and ~25 μm. Nevertheless, they did not observe the slight, but clear, decrease in the mean grain sizes, at 142 cm depth in core GS05.

The grain size decrease occurs before the major change in magnetic susceptibility (Fig. 3), which was related to a lowering of the CS level due to the decrease of the meltwater supply into the basin. This granulometric change thus suggests most probably an earlier decrease in the water supply from the catchment area.

Based on sediment description, radiocarbon and other proxies such as the carbonates, an overlap is possibly suggested between the top of core GS05 (station 2) and the bottom of core CP14 (station 6, 55 km north of GS05 and shallower) (Leroy et al., 2007 and here).

4.3. Pollen and spores and NPP in core GS05

Six pollen zones have been identified after CONISS analysis. Pollen zones P-5 to 6 are attributed to chronozones based on the age–depth model. For pollen zones P-1 to P-4, palynozones are suggested rather than chronozones.

4.3.1. Zone P-1, 305–135 cm: Last Glacial period

This long and homogeneous zone is dominated by Amaranthaceae–Chenopodiaceae (A–C) with 40–50% and by *Artemisia* with 30–40% (Fig. 4). The reconstructed vegetation around the CS is desertic in the driest places such as the eastern shores, and steppic in more favourable microclimates of the Caucasus and Elburz Mountains. The regular presence of Plumbaginaceae, a salt-tolerant family, suggests the existence of saltmarshes.

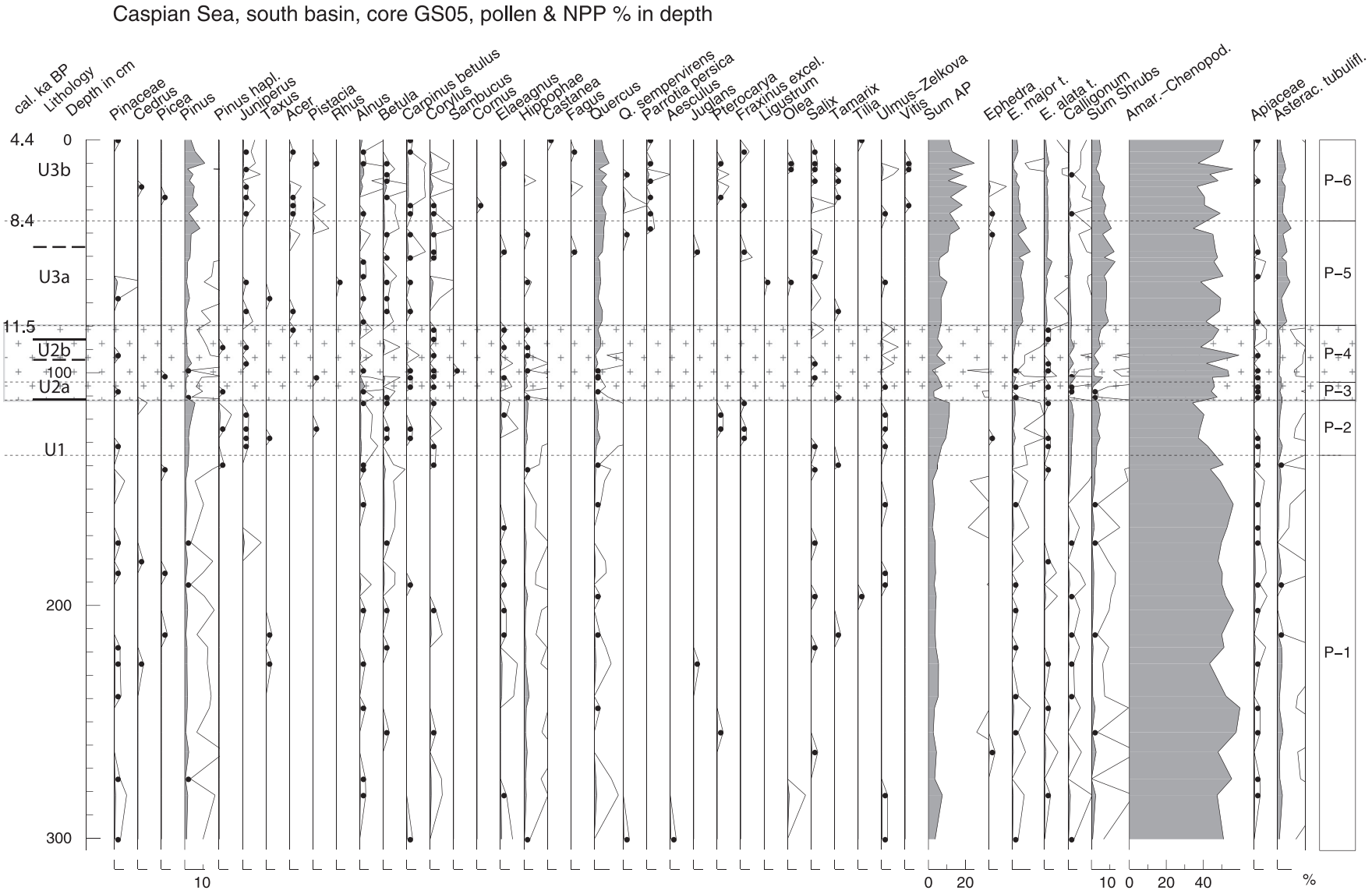

Fig. 4. Pollen and spore diagram of core GS05. The horizontal box with crosses highlights the Younger Dryas stadial. 10× exaggeration curves and dots for values lower than 0.5%.

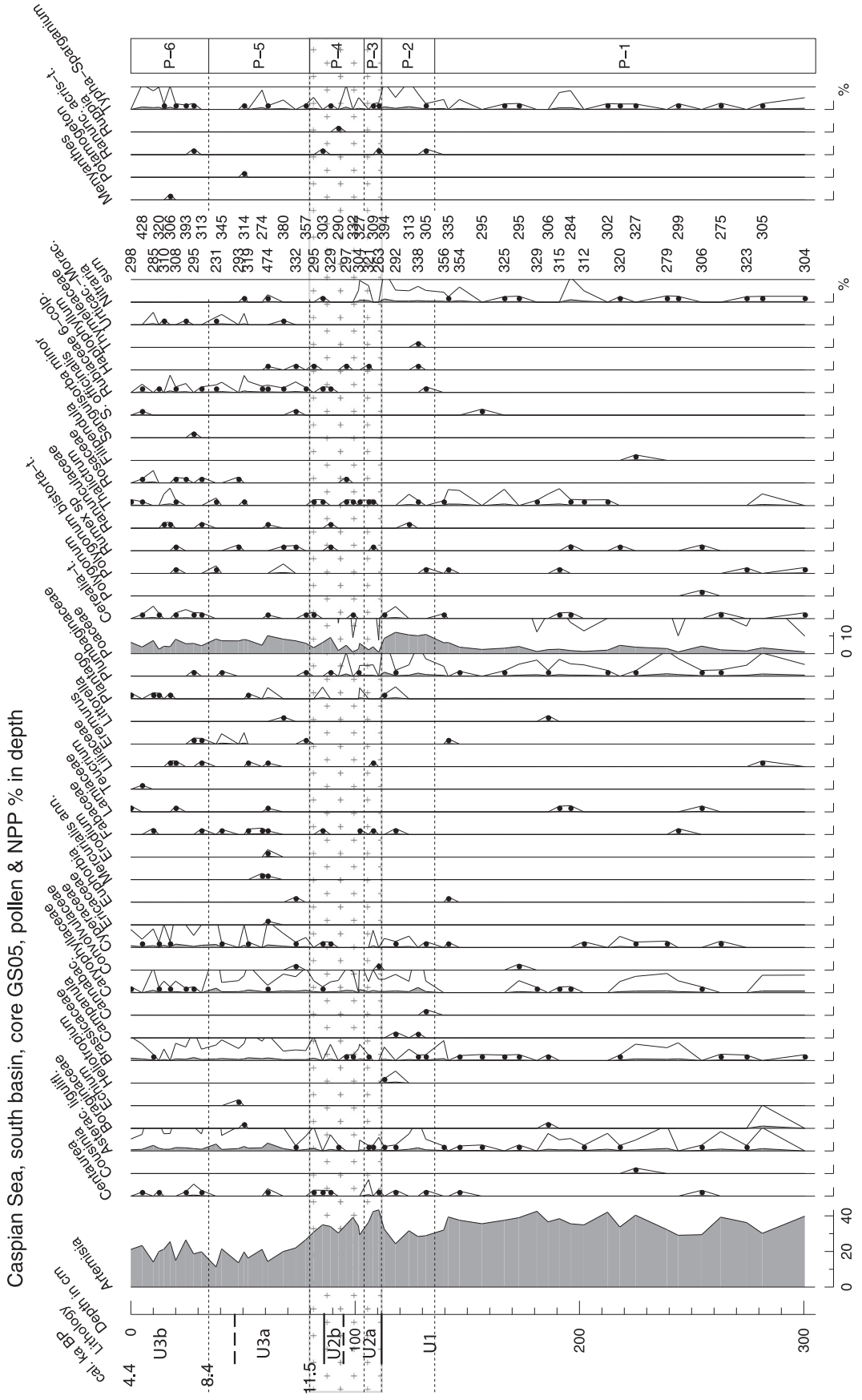

Fig. 4. (*continued*).

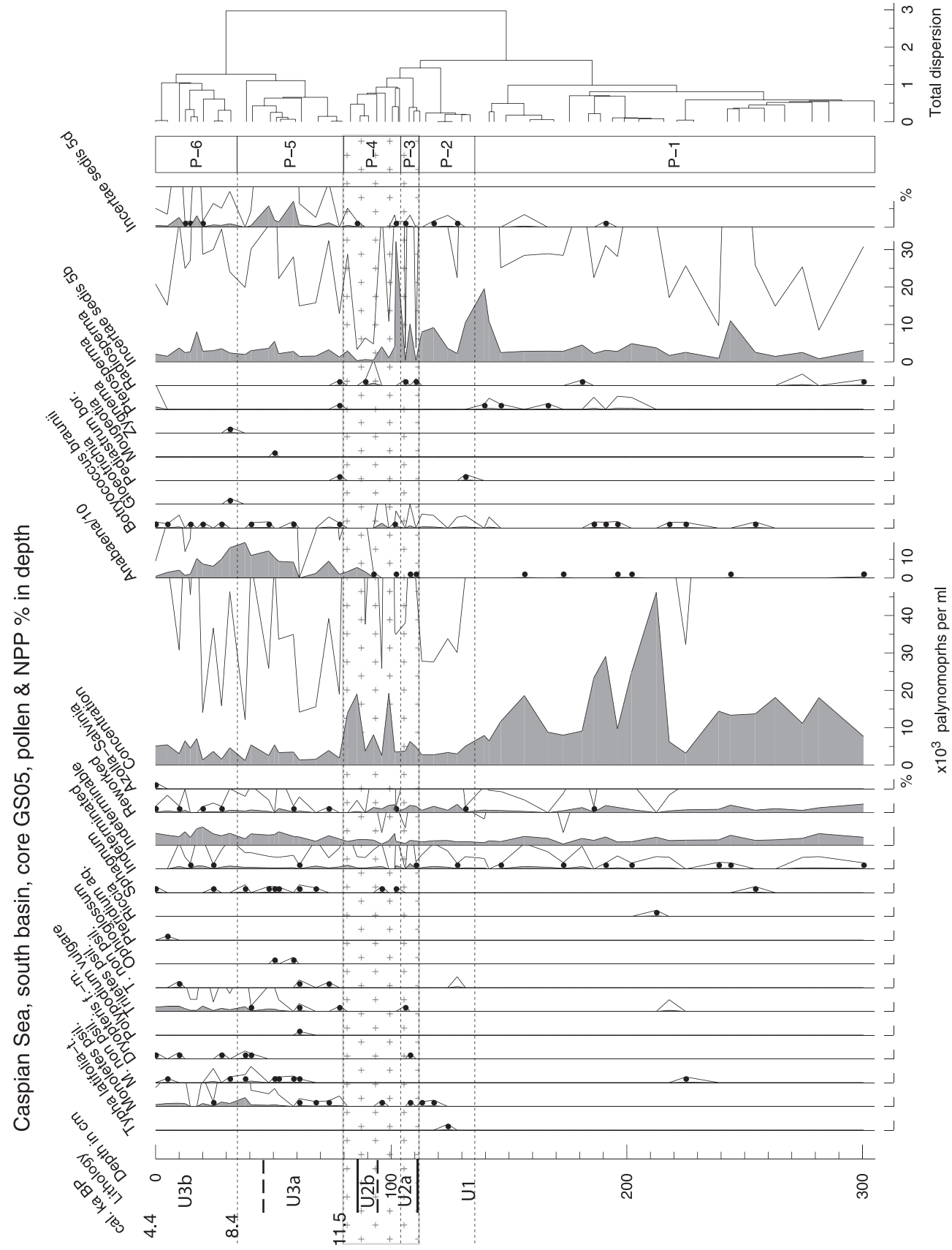

Fig. 4. (*continued*).

Arboreal pollen (AP) is very rare and only *Betula* is frequent, especially in the upper part of this zone. The microfossil of the green algae *Pterosperma* frequently occurs in the upper part of this zone too.

Concentration values are high and this is most likely due to strong winds transporting pollen to the centre of the basin. Moreover, this occurs despite extremely high sedimentation rates suggested by the high amount of detritics and the anomalous and stable radiocarbon dates.

4.3.2. Zone P-2, 135–111.75 cm: Allerød palynozone

This zone is characterised by a small, but significant, increase of the AP percentages, especially of *Pinus, Juniperus*, *Alnus*, *Quercus*, *Elaeagnus*, and *Hippophae*, and the shrub *Calligonum*. More remarkably, warm-loving species such as *Pterocarya* and *Fraxinus* make a brief appearance. Amongst the non-arboreal pollen (NAP), A–C (40%) and *Artemisia* (25%) are the dominants, but it is worth mentioning regular occurrences of *Nitraria* (a salt-tolerant plant), a maximum of Poaceae and the continued presence of Plumbaginaceae. *Botryococcus* occasionally occurs. Concentrations carry on falling. This zone of climatic improvement is attributed to the Allerød palynozone.

4.3.3. Zone P-3, 111.75–104 cm: Younger Dryas palynozone, part 1

This short zone (3 samples) stands out by its minimum of AP and shrubs and by the maximum of *Artemisia* (≥42%). It is similar to zone P-1, if not colder. *Botryococcus* is still occasionally present. *Radiosperma corbiferum*, of unknown origin, often found in low salinity environments (Sorrel et al., 2006), is mostly observed here and in the following zone. Concentrations are low. This zone of climatic deterioration is attributed to the Younger Dryas palynozone.

4.3.4. Zone P-4, 104–79.75 cm, until 11.5 cal. ka BP: Younger Dryas palynozone, part 2

Elaeagnus, *Hippophae* and *Calligonum* continue to be regularly present. *Quercus* values recover after zone P-3. Some rare occurrences of *Ulmus-Zelkova* are noteworthy. However AP values are still lower than during the Allerød. The last significant presence of *Nitraria* is found at the transition P-3 to P-4. The percentages of *Artemisia* are still high but are on a decreasing trend. Plumbaginaceae starts fading away. Poaceae are still at the low abundances of the preceding zone.

As *Botryococcus* becomes less frequent, *Anabaena*, a cyanobacteria that thrives in nitrogen-limited environments (Räsänen et al., 2006), starts its development. Pollen and spore concentrations recover to values close to 10,000 grains per ml. Quite clearly, this is still a very dry phase, but the saltmarsh extension is decreasing.

4.3.5. Zone P-5, 79.75–34.75 cm, from 11.5 to 8.4 cal. ka BP: "Shrub phase" Holocene

Pinus and *Quercus* progressively recover to values not seen since the end of the Allerød. At the very end of this zone, several warm-loving deciduous trees start appearing: *Acer*, *Carpinus betulus* and *Parrotia persica*. AP values progressively increase throughout this period.

Ephedra major-t. displays high values (>4%). *Calligonum* and *Ephedra alata*-t. have continuous curves, while *Elaeagnus* and *Hippophae* have quasi disappeared.

Artemisia values notably decrease, while Asteraceae and Cyperaceae become more frequent. Rubiaceae maintain their regular presence started at the end of the previous zone. Spores of *Sphagnum* are more regular in this zone. Psilate trilete spores become frequent in the second half of the zone, probably reflecting the development of some woodlands and forests. *Anabaena* has values that reach a maximum at the end of this zone. Incertae sedis 5d (illustrated in plate 1 of Leroy, 2010) start their regular occurrence.

Because of the abundance of several shrub taxa, this zone is called a shrub phase, and because of the chronology, it is attributed to the beginning of the Holocene.

4.3.6. Zone P-6, 34.75 cm-top, from 8.4 to 4.4 cal. ka BP: "Tree phase" Holocene

The maximum of several tree taxa, such as *Pinus*, *Juniperus*, *Alnus*, *C. betulus*, *Quercus* and *P. persica*, is seen in this zone. The occurrence of the latter is significant as it has a geographical distribution restricted to the Hyrcanian vegetation in the Elburz Mountains and its presence therefore unequivocally indicates both an efficient transport from the south and the development of large forests on these mountains. *Acer* and *Vitis* appear while *Pterocarya* re-appears. In the most favourable areas around the south basin of the CS, forests have established themselves. In this case, *Pinus* pollen was not transported by the Volga as a weak river influence to the coring site is reconstructed, e.g. by the low values of reworked elements. Moreover the source of *Pinus* pollen could be *P. eldarica*, a tree that grows in Azerbaijan and Georgia (Weinstein, 1989; Leroy et al., 2013a).

Table 3
Factor loadings for pollen (upper part) and dinocyst (bottom part) taxa included in the two PCA done in this study. For pollen, data is from GS05 core; while for dinocysts, data is from GS05 and CP14 cores. Numbers in bold and italics indicate taxa with large factor loadings.

Pollen GS05	PC1-Pollen	PC2-Pollen	PC3-Pollen
Calligonum	***0.85***	−0.15	−0.05
Poaceae	***0.83***	0.02	0.19
Sum shrubs	***0.78***	0.48	0.15
Ephedra major-t.	***0.64***	***0.60***	0.12
Caryophyllaceae	***0.62***	0.04	0.07
Brassicaceae	***0.51***	0.25	0.23
Amaranthaceae-Chenopodiaceae	−***0.70***	0.11	−0.43
Asteraceae tubuliflorae	0.43	***0.61***	0.17
Ephedra alata-t.	0.35	***0.58***	0.34
Quercus	0.49	***0.52***	0.48
Artemisia	−***0.52***	−***0.54***	−0.31
Nitraria	0.17	−***0.76***	−0.16
Hippophae	−0.13	−***0.84***	−0.20
Plumbaginaceae	0.05	−***0.84***	−0.02
Sum Trees	0.45	0.21	***0.72***
Juniperus	0.29	0.08	***0.69***
Pinus	0.40	0.10	***0.67***
Quercus sempervirens	−0.04	0.10	***0.67***
Parrotia persica	−0.06	0.34	***0.67***
Cyperaceae	0.35	0.32	***0.53***
Carpinus betulus	0.02	0.35	***0.51***
Pinaceae	−0.07	−0.06	−0.04
Alnus	0.00	0.04	0.16
Betula	0.16	0.19	0.07
Corylus	0.04	0.09	0.05
Salix	0.24	0.15	0.07
Asteraceae liguliflorae	0.39	0.36	0.24
Boraginaceae	0.01	−0.06	−0.11
Dinocysts GS05 & CP14	**PC1-dinos**	**PC2-dinos**	**PC3-dinos**
Lingulodinium machaerophorum	***0.90***	0.03	0.04
Pentapharsodinium dalei	***0.88***	0.03	−0.23
Caspidinium rugosum	***0.84***	0.30	−0.02
Pyxidinopsis psilata	−***0.83***	0.24	0.08
Spiniferites cruciformis A	0.00	***0.78***	−0.35
Spiniferites cruciformis C	0.26	***0.74***	−0.27
Impagidinium caspienense	0.09	−***0.96***	0.04
Spiniferites belerius	−0.31	−0.15	***0.70***
Brigantedinium	0.00	−0.37	***0.60***
Caspidinium rugosum rugosum	−0.44	0.42	***0.59***
Spiniferites cruciformis B	−0.32	0.41	−***0.68***

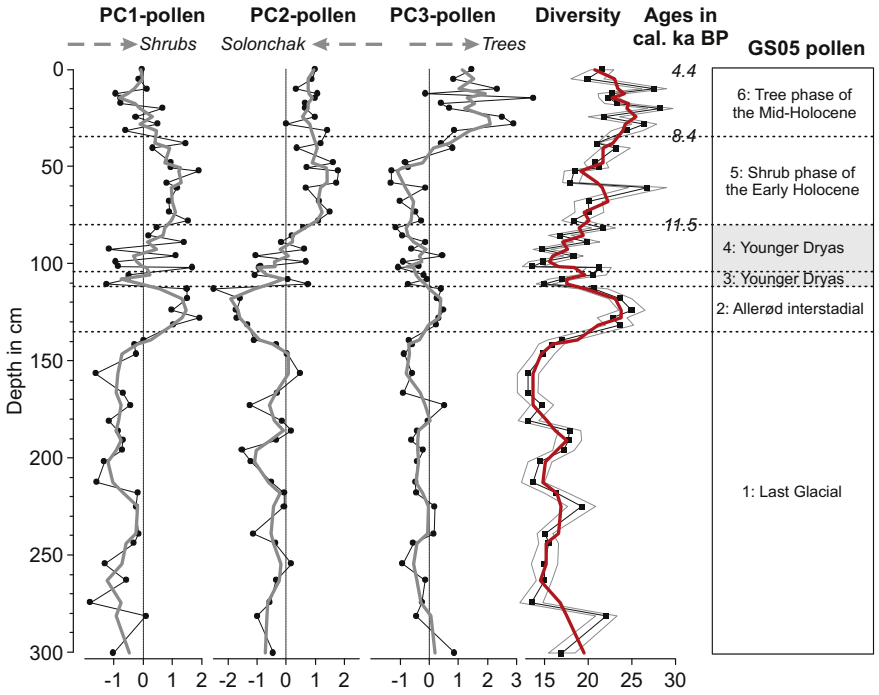

Fig. 5. Factor scores for the first three principal components of the pollen data in GS05 core and results of rarefaction analysis. A 3-sample running average has been added to each graph.

Shrub percentages progressively decrease throughout the zone. *Cerealia*-t. shows a maximum, but this cannot be attributed to agriculture since domesticated cereal grains cannot be distinguished from a wild Poaceae genus, *Aegilops*, that also has a large pollen grain and lives in the area. Various spores are common (but not *Sphagnum*). *Anabaena* values progressively decrease throughout this zone.

4.4. Pollen: PCA and diversity

Seven principal components account for the 72.5% of the variance. PC1 explains 18.8%, PC2 16.2%, while PC3 13.7%. The rest of the principal components are related with the variance of single pollen types and represent a very small proportion of the total variance.

In PC1-p, *Calligonum*, Poaceae, the sum of shrubs, *E. major*-t., Caryophyllaceae and Brassicaceae show high positive loadings, while A-C and *Artemisia* show high negative loadings (Fig. 5 and Table 3). Thus, this component presents positive scores in samples where shrubs and some herbs are important, and negative scores in samples where desertic/steppic vegetation is the dominant. Factor scores are positive during zones P-2 (Allerød) and P-5 (Early Holocene shrub phase), negative during zone P-1 (Last Glacial) and close to zero during zones P-3, P-4 (Younger Dryas) and P-6 (Mid-Holocene tree phase) (Fig. 5), highlighting the development of shrub formations during periods of climate improvement at the Allerød and the Early Holocene.

In PC2-p, Asteraceae tubuliflorae, *E. major*-t., *E. alata*-t. and *Quercus* show high positive loadings, while Plumbaginaceae, *Hippophae*, *Nitraria* and *Artemisia* show high negative loadings (Table 3). Thus, this component presents negative scores in samples reflecting the development of saltmarshes and solonchak, and positive scores in samples where terrestrial vegetation with better drained soils developed. Factor scores are mainly negative from zones P-1 to 4, and positive in P-5 and P-6 (Fig. 5), pointing out at a large shift between the Late Pleistocene and the Holocene.

Finally, in PC3-p the sum of trees, *Juniperus*, *Pinus*, *Quercus* sempervirens, *P. persica*, Cyperaceae and *C. betulus* present high positive factor loadings (Table 3). This component shows positive scores in samples where more humid and warmer conditions allowed the development of trees and sedges. It happens mainly during zones P-2 (Allerød) and P-6 (Mid-Holocene tree phase).

Palynological richness is low in zone P-1, rises abruptly in P-2, while in P-3 and P-4 drops. It shows higher values from P-5 onwards, and is maximal during P-6 (Fig. 5). Thus, palynological diversity is lower during cold phases (Last Glacial and Younger Dryas) and higher during warmer periods (Allerød and Holocene).

4.5. Dinocysts in core GS05

4.5.1. Zone D-1, 305–129.75 cm: Khvalynian highstand

The spectra are largely dominated by *Impagidinium caspienense* (50%) (Fig. 6). *I. caspienense* is a relatively new species whose ecology is unknown. However because high values have been obtained in surface samples (Kazancı et al., 2004; Leroy et al., 2013a, 2013b) and in Holocene cores of the CS (Leroy et al., 2007, 2013a, 2013b), *I. caspienense* must be a species of relatively low salinities, probably 13 psu, in comparison to other species of the same genus.

Secondary taxa of lower salinities are however abundant *Pyxidinopsis psilata*, *Spiniferites cruciformis* A and *Caspidinium rugosum rugosum*. *P. psilata* and *S. cruciformis* are dominant in Early Holocene sediments from the Black Sea and have been related to slightly brackish conditions (<7 psu) and usually cool waters (Wall et al., 1973; Mudie et al., 2002; Filipova-Marinova et al., 2013), although the scarcity of modern analogues does not readily permit the delimitation of their ecological affinities (Marret et al., 2004). *S. cruciformis* has also been observed in lakes, such as in the Lateglacial sediment of Lake Kastoria, Northern Greece, and in the top cm of Lake Sapanca sediment cores (NW Turkey) (Leroy and Albay, 2010). Three forms of *S. cruciformis* have been recorded separately

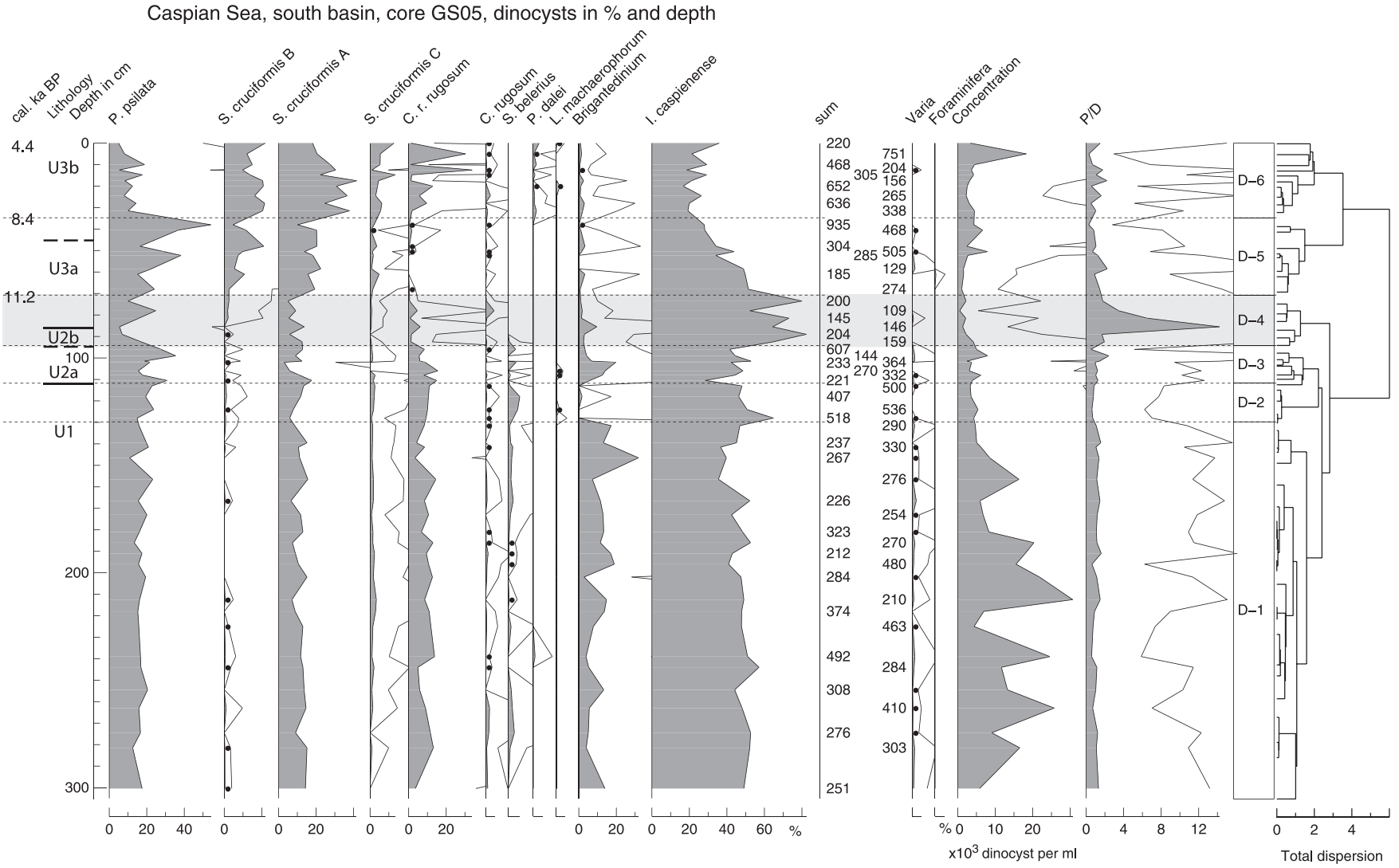

Fig. 6. Dinocyst diagram of core GS05. The horizontal grey box highlights the Mangyshlak lowstand. 10× exaggeration curves and dots for values lower than 0.5%.

(forms A, B and C) (Marret et al., 2004). *C. r. rugosum* and *C. rugosum* are two forms of a new genus about which not much is known yet. In the Marmara Sea, the genus occurs during periods of meltwater fluxes (Londeix et al., 2009). Its ecology is suggested from its frequent association with low salinity taxa.

Towards the end of this zone, values of *Brigantedinium*, which are fluctuating around 10%, increase. *Brigantedinium* species are ubiquitous; they are present from low to high latitudes, and from neritic to open ocean regions. They are often related to high nutrient richness.

Spiniferites belerius displays a quasi–continuous curve. This is a neritic marine species, from temperate to tropical seas. In the CS, several specimens with a form intermediate between *S. belerius* and *I. caspienense* have been found. Bradley et al. (2012) consider this taxon as a species typical of periods of transitions in salinity and water temperature in the Black Sea. Concentrations are maximal in this zone: often higher than 10,000 cysts per ml. The *P*/*D* ratio is low as expected for an open sea site (see modern samples in Leroy et al., 2013a).

4.5.2. Zone D-2, 129.75–111.75 cm: Khvalynian highstand with *S. belerius*

This zone is fairly similar to the preceding one, notwithstanding a dramatic drop of *Brigantedinium* and a significant maximum of *S. belerius*. Concentrations drop to c. 5000 cysts per ml.

4.5.3. Zone D-3, 111.75–94.25 cm: Khvalynian highstand

This zone shows a return to the conditions of zone D-1.

4.5.4. Zone D-4, 94.25–70.75 cm, until 11.2 cal. ka BP: Mangyshlak lowstand with *I. caspienense*

I. caspienense reaches maximal values, often higher than 70%. Concurrently the values of many taxa, such as *P. psilata*, *C. r. rugosum* and *Brigantedinium*, decrease. *S. belerius* has disappeared and

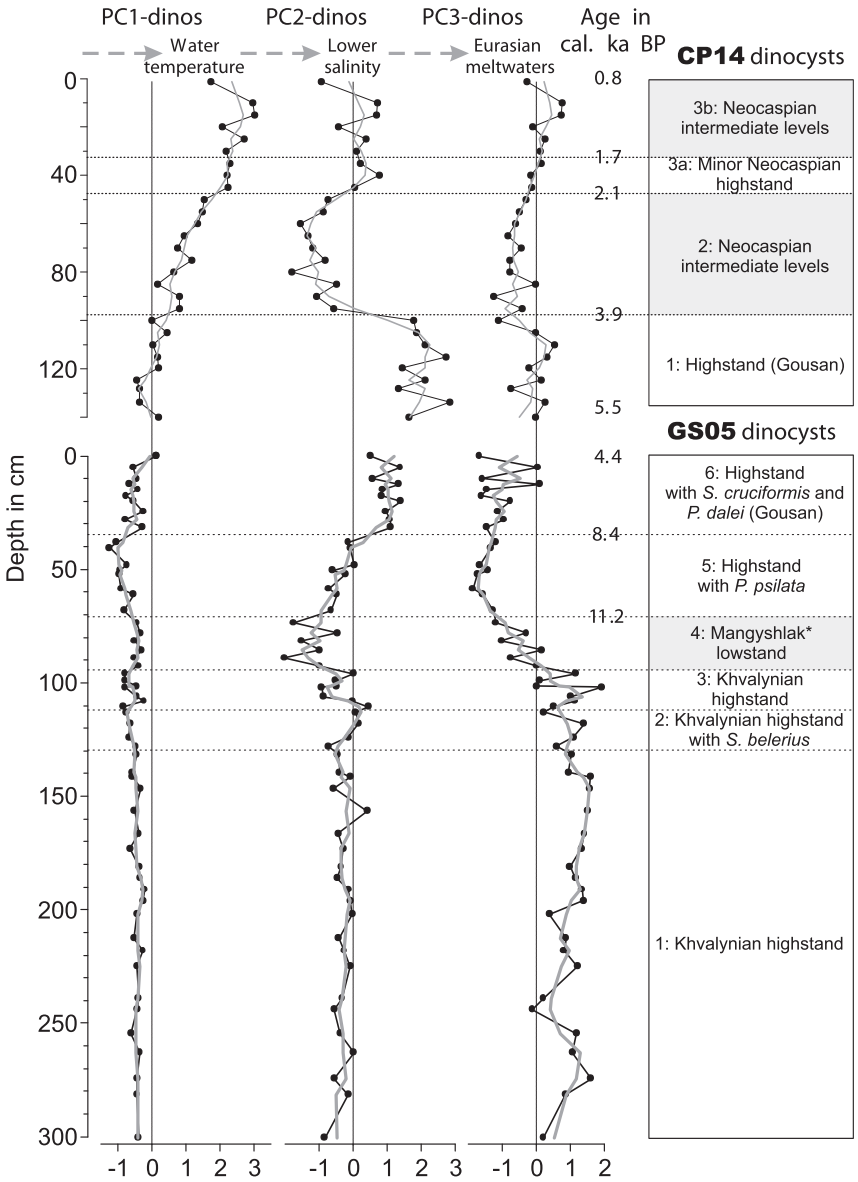

Fig. 7. Factor scores for the first three principal components of the dinocyst data in GS05 and CP14 cores. A 3-sample running average has been added to each graph. Suggested links to the Russian stratigraphy (Mangyshlak lowstand according to Mayev (2010) and Sorokin (2011); Gousan highstand according to Svitoch (2012) and to the CP14 sequence (Leroy et al., 2007)). * Enotaev lowstand according to Svitoch (2012).

will not return in this sequence. Dinocyst concentrations are low and decrease upwards to a minimum. The *P*/*D* ratio is maximal indicating a clear influence of the continent on this location in the centre of the south basin with plants growing on the newly emerged shores. Water salinity, the highest of the sequence, is similar or even higher to that of the present day CS.

4.5.5. Zone D-5, 70.75–34.75 cm, from 11.2 to 8.4 cal. ka BP: Highstand with P. psilata

P. psilata percentages are maximal, reaching progressively up to 40%. *S. cruciformis* B started to develop, while *S. cruciformis* A and B increase. *I. caspienense* starts a slow decreasing trend continuing until the core top. Concentration is at first very low and then increases slightly across this zone. The *P*/*D* ratio has gone back to its average values around 1.2. The salinity is suggested to be again low.

4.5.6. Zone D-6, 34.75 cm-top, from 8.4 to 4.4 cal. ka BP: Gousan highstand with S. cruciformis

The three forms of *S. cruciformis* reach maximal values. *I. caspienense* values are minimal. *P. psilata* percentages further decrease. *Pentapharsodinium dalei* values are quasi continuous. *P. dalei* is a cold, euryhaline, Arctic cyst, with an affinity for environments of strong seasonal thermal contrast (Marret and Zonneveld, 2003). In the CS, it is however abundant in the Holocene (Leroy et al., 2007).

Lingulodinium machaerophorum with very low values starts to be noticeable in the last sample. *L. machaerophorum* highest abundance is often found in neritic environments, where winter sea-surface temperatures are above 12 °C. This species is known for its euryhaline nature. While in the Black/Marmara seas, it has been present since at least the LGM (Londeix et al., 2009), in the CS it appears only c. 3200 calibrated years ago (Leroy et al., 2013a, 2013b).

This zone illustrates a period of low salinity, but under other conditions than zone D-5. The difference between the two low salinity zones cannot be explained easily because of the scarcity of modern analogues does not allow us to define well the limits of their ecological affinities. A possible reason is that *P. psilata* may live in colder waters than *S. cruciformis*; and therefore the D-5/6 transition is likely caused by warming of relatively fresh waters.

4.6. Dinocysts: PCA

For the PCA analysis, both the data from core GS05 and core CP14 are combined (Leroy et al., 2007). Three principal components account for 73.5% of the variance. PC1 explains 31.3%, PC2 24.7%, while PC3 17.5%.

In PC1-d, *L. machaerophorum*, *P. dalei* and *C. rugosum* show high positive loadings, while *P. psilata* shows a high negative loading (Table 3). Factor scores are negative in GS05 core, while in CP14 scores are low at the beginning and develop a trend to high scores up to the top (Fig. 7). We hypothesize that this PC reflects an increase of surface water temperature.

In PC2-d, *S. cruciformis* A and B show high positive factor loadings, while *I. caspienense* shows a high negative loading (Table 3). Thus, this component presents negative scores in samples reflecting low salinity waters (13), and positive scores in samples where waters are more brackish/fresh (7). Factor scores are close to zero from zones D-1 to 3, D-5 and Dz14-3a and 3b, negative in D-4 and Dz14-2, and positive in D-6 and Dz14-1 (Fig. 7), pointing out higher salinities during lowstand periods, and brackish/freshwater conditions during highstands.

Finally, in PC3-d *S. belerius*, *Brigantedinium* and *C. r. rugosum* present high positive loadings, while *S. cruciformis* B shows a high negative loading (Table 3). This component shows positive factor scores from zones D-1 to 3, negative scores from D-4 to 6, and variable, but close to zero values in CP14 core (Fig. 7). This component is difficult to interpret, but we think it could be related to changes in the source of water input (see discussion).

5. Discussion

5.1. Lithology and age–depth model

A reliable chronology starts at 86 cm, i.e. 11.8 cal. ka BP. This is very close to the main change in the pollen diagram at 80 cm (P-4/5 boundary) at 11.5 cal. ka BP and it is in the middle of dinocyst zone D-4, which is the Mangyshlak lowstand.

The sedimentation rate obtained for the sequence varies between 10 and 30 cm/ka for the Late Pleistocene-Early Holocene and 7 and 10 cm/ka above 10.3 cal. ka BP (Fig. 2).

A progressive increase of carbonate content was observed in other cores across the Mangyshlak period from the eastern shelf of the CS (Mayev, 2010). The increase of the carbonate production in the CS seems to have been triggered by the temperature increase at the very Early Holocene (Pierret et al., 2012), as it has also been seen in the Black Sea (Bahr et al., 2005).

The Black Sea has a problem of reservoir effect (up to 1000 years for the deep sea cores) (Bahr et al., 2005), with moreover an input of dead carbon that is not time stable. The CS most likely suffers from the same problem: with varying river inflows and sources and with varying aeolian inputs, such as via sandstorms from the east (southern Turkmenistan) where limestone formations occur (Lahijani and Tavakoli, 2012). The reservoir estimation in the Black Sea was made by comparison between cores, one dated on ostracods mixed with shell debris with one that was dated only on adult mollusc shells (Bahr et al., 2005).

5.2. Pollen-inferred vegetation

5.2.1. The Late Pleistocene

For core GS05, the PCA has shown that the factor explaining a high percentage of the variance of the pollen dataset is the abundance (or not) of shrubs that negatively correlate with the abundance of desertic/steppic taxa. Therefore the development of shrubs is clearly the most important change in this pollen diagram. An increase in the importance of shrubs during the Allerød contrasts with the desertic/steppic vegetation reconstructed for the Last Glacial and the YD (PC1-p, Fig. 5), showing a clear climate improvement during this interstadial. Moreover, PC3-p has a local peak, meaning that some trees were also important during this warmer period of the Late Pleistocene.

In diagrams of the Marmara Sea (Valsecchi et al., 2012) and in the east of the Black Sea (Shumilovskikh et al., 2012), the period before the Bølling–Allerød interstadial is characterised by an open landscape with the presence of bushes such as *Hippophae* and *Ephedra*. The YD is defined by an increase of *Artemisia* and a drop of deciduous *Quercus* pollen. The YD on the Iranian Plateau (Bottema, 1995) is similarly identified by an aridification. These observations are very comparable to those of the GS05 record.

In a pollen diagram from the Siculo-Tunisian strait (Desprat et al., 2013), the Late Pleistocene and the YD are both characterised by high values of *Artemisia* and *Ephedra*. This major difference with the GS05 sequence is probably due to the much colder conditions in S–W Asia than in the south-central Mediterranean area.

5.2.2. The Early Holocene

A shift in salt tolerance vegetation is marking the onset of the Holocene. PC2-p shows negative or close-to-zero scores during the

Late Pleistocene (Fig. 5), while they are positive during the Holocene, reflecting a shift from saltmarshes to terrestrial vegetation on better drained soils.

Zone P-5, spanning from 11.5 to 8.4 cal. ka BP, illustrates a new shrub phase (*Ephedra* and *Calligonum*), and PC1-p scores reach similar values to the ones showed during the Allerød (Fig. 5). *Pinus* and *Quercus* dominate the relatively low arboreal percentages, with only sparse occurrences of other trees. The beginning of tree development is somewhat late and delayed by 3.1 ka BP compared to the Pleistocene–Holocene warming, as it is only after 8.4 cal. ka BP that trees, other than *Pinus* and *Quercus*, appear in the diagram with continuous curves. This forest development is reflected by PC3-p, showing the largest scores of the entire record (Fig. 5).

This forest delay is typical of other sites in the SE Mediterranean region and in the Middle East. In Lake Urmia, Northern Iranian Plateau and other lakes of the Middle East (Zeribar and Van), the oak forest development is delayed to 7.5 or even c. 6.5 cal. ka BP (Djamali et al., 2008). In southern Georgia, the *Quercus* maximum is late and comes a millennium later than in Lake Van, although the record of Lake Aligol shows a nice progressive expansion of trees straight from the beginning of the Holocene (Connor, 2006). In the Black Sea (e.g. Shumilovskikh et al., 2012), besides *Pinus* and *Quercus*, trees start to develop only after 8.5 cal. ka BP, roughly at the same time as in the CS surroundings. However, some other sites do not show this delay, such as a Marmara Sea sequence (Valsecchi et al., 2012). The latter site and a sequence in the southeast corner of the CS are both close to LGM tree refugia (Leroy and Arpe, 2007; Arpe et al., 2011), explaining why the arboreal vegetation could react so fast to the Holocene warming.

Wright et al. (2003) suggested that this Early Holocene dry period extended between Bulgaria and at least the CS (maybe as far as the Altai Mountains). The causes they suggested are increased summer temperatures and insolation over an area too far inland from sources of moisture. To this, one may also add the occurrence of two large water bodies filled by cold meltwater, the CS and the Black Sea, which may have had negative feedback on regional climates via the "lake effect" delaying the Early Holocene warming (Small et al., 2001).

The correlation with the bottom zone of core CP14, Pz14-1 (Fig. 8), is not completely satisfying as some differences occur, such as in the higher amount of *Pinus*, Asteraceae tubuliflorae and

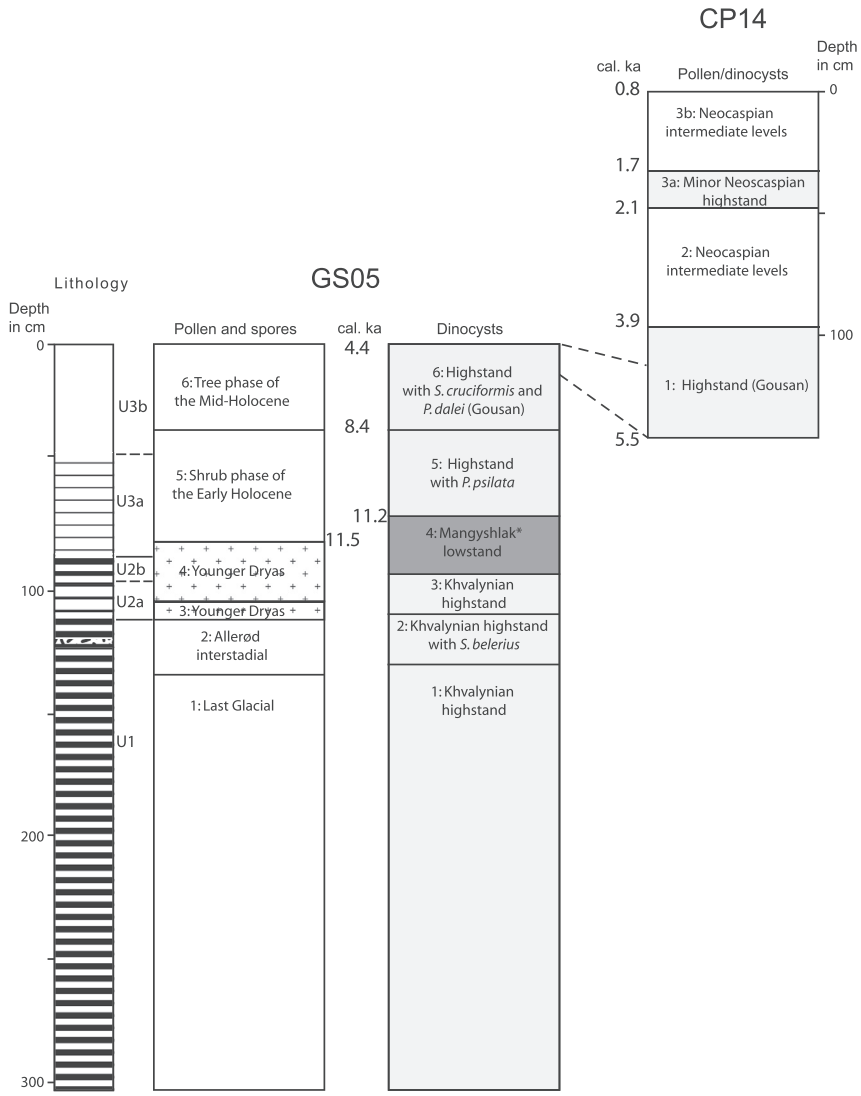

Fig. 8. Comparison of the pollen and the dinocyst zones of core GS05, suggested links to the Russian stratigraphy (Mangyshlak lowstand according to Mayev (2010) and Sorokin (2011); Gousan highstand according to Svitoch (2012)) and to the CP14 sequence (Leroy et al., 2007). * Enotaev lowstand according to Svitoch (2012).

liguliflorae, spores and massula of *Salvinia* in the CP14 diagram (Leroy et al., 2007). These are mostly water-transported taxa and may reflect the shallower water depth of core CP14 (Fig. 1B) and the subsequent difference in the bottom currents inputs to the sediments.

5.3. Dinocyst-inferred water levels

5.3.1. Differences between deep sea and coastal assemblages

The general low salinity signal of the GS05 sequence (<7 psu) is interrupted by a more brackish phase (c. 13 psu or more): zone D-4, recording the Mangyshlak lowstand, where PC2-d factor scores are negative (Fig. 7). In CP14, negative scores occur during Pz14-2, a phase related to the intermediate levels of the Neocaspian period. This is either because the salinity was higher and similar to the Mangyshlak lowstand as recorded in the sequence GS05, and in this case this would fit the lowstand history recognised by Svitoch (2010) who highlights important lowstands in the Holocene; or because the CP14 site, being in a slightly shallower position than GS05, is more sensitive to water level lowering. A combination of both is likely. Because core GS05 has been taken at a deep-water depth, it is possible that only the main events are recorded owing to a buffering due to deep water depths and distance to the shores. A regression/transgression might have been recorded earlier/later or longer/shorter in the margins of the CS.

A comparison with the dinocysts diagram of **core TM** in a lagoon of the SE corner of the CS underlines some essential differences. In the TM palynological diagram, which starts at 10.6 cal. ka BP, the dinocyst assemblages are already dominated by *I. caspienense* (Leroy et al., 2013a). The low salinity taxa are relatively rare, for example *P. psilata* is quasi absent to the contrary of core GS05. *S. cruciformis* values remain at low levels. *P. dalei* develops low percentages only after a hiatus at c. 3.9 cal. ka BP. Hence, the difference indicates that the sequence from the SE corner of the CS reflects more saline Holocene conditions than the deep basin core GS05. This is most likely due to its location in much shallower waters, i.e. in a coastal lagoon, with higher evaporation and temperature making it more sensitive (Fig. 1A).

The comparison between the dinocyst assemblages in the three sites confirms what has been suggested earlier (Leroy et al., 2013a), that the Khvalynian, Mangyshlak and Neocaspian stages should be considered as biozones rather than chronozones, due to the important role of the distance from the coast.

5.3.2. The glacial and Lateglacial periods

The highstand of the Khvalynian is marked by a combination of slightly brackish taxa and more brackish taxa with a small peak of *S. belerius* in the Allerød interstadial (PC2-d, Fig. 7). *S. belerius* shows a clear presence until before the Mangyshlak lowstand in core GS05 (zone D-3).

S. belerius displays a peak at 7.6–7.0 cal. ka BP in the western Black Sea (Bradley et al., 2012) and at 8.4–7.0 cal. ka BP in the eastern Black Sea (Shumilovskikh et al., 2013), therefore later than in the south basin of the CS. However in the Marmara Sea, *S. belerius* displays maximal values already in the YD period (Londeix et al., 2009).

5.3.3. The Mangyshlak lowstand

Dinocyst zone D-4 (finishing at 11.2 cal. ka BP), with the strong increase of *I. caspienense* percentages, low concentrations, a high *P/D* ratio (higher influence of the continent) and PC2-d negative scores (Fig. 7), is attributed to an increase in salinity and to the decrease of the water level. This is, according to the chronology of GS05, attributed to the Mangyshlak lowstand, as defined by Mayev (2010) and Sorokin (2011). However Svitoch (2012) calls it the Enotaev lowstand and keeps the name of Mangyshlak for a later lowstand.

Here is the first time that the Mangyshlak lowstand is highlighted in the set of cores taken in the 1994 cruise (Kuprin and Pirumova, 2002), perhaps due to the type of proxies and/or the time resolution.

In **core TM** from the SE corner of the CS, the Mangyshlak lowstand is clearly shown by a hiatus at the transition of zones TM1/2, i.e. somewhat close to the Pleistocene–Holocene transition, and due to, as mentioned above, its location closer to the shoreline.

This lowstand must have been caused more than just by climatic change: a change in the palaeohydrology of the two main rivers, i.e. Volga and Amu Darya, must have occurred briefly. In fact, PC3-d shows a clear shift at the D-3/4 boundary (Fig. 7), which has been interpreted as a change in the Eurasian meltwaters that would have influenced the hydrological inputs in the CS.

It is interesting to note that, in the Black Sea, a lowstand is reconstructed for the period from 14.7 to 10 ^{14}C ka BP (Hiscott et al., 2007), therefore the dinocyst zone attributed to the Mangyshlak in the CS overlap the end of this Black Sea lowstand. The water level lowering was suggested to be due to evaporation in the case of the Black Sea.

5.3.4. The last highstand

D-5 indicates water salinities similar to those during the Khvalynian highstand (D-1–3), with PC2-d scores close to zero. However, zone D-6 presents a higher contribution of low salinity taxa and shows fresher waters than in the Khvalynian highstand, and has been interpreted as the Gousan highstand in GS05. If the salinity can be taken as a relatively direct sea level indicator, this would mean that zone D-6 has the highest levels of the sequence, and that it is very likely that the CS was overflowing its sill to the Black Sea.

Preliminary data from the Volga delta (Hoogendoorn et al., 2010) and Gorgan delta (Kakroodi et al., 2012) and a partial Holocene sequence from a lagoon in the SE corner of the CS (Leroy et al., 2013a) are not incompatible with a highstand, although the durations are not identical. These data however are questionable as these sequences are formed in a dynamic, noisy, deltaic environment or in coastal area with no sedimentation during lowstands and erosion at the changes of water levels, instead of a continuous fine-grained deep-sea setting. Moreover in order to explain any potential difference between the north/middle and the south basins, it is not impossible that the Apsheron sill (Fig. 1B) played some role in isolating the south basin (unpublished work on a core in the middle basin using dinocysts by one of the present paper's authors).

It is not precisely known when meltwater stopped flowing south from the Eurasian ice sheet to the Aral/Caspian system, but most likely well before 10 ^{14}C ka BP (Lambeck, 1996). Therefore one would need to invoke another source of water to maintain such high levels. The Amu Darya, that flows from the Pamirs, has been suggested as an important source of water for the CS (Kes, 1995; Ferronsky et al., 1999; Leroy et al., 2007, 2013a). Thus, PC3-d negative scores could be indicative of this shift from Eurasian meltwater to Pamir water input (Fig. 7). The Amu Darya sources are largely in Tajikistan, where it is called the Panj River (UNEP et al., 2011). It receives water from the melting of glaciers. The modern Tajikistan is the wettest of the central Asian republics with mountainous regions (the Pamirs) receiving in some places more than 1500 mm of precipitation per year during western disturbances (Syed et al., 2006) (Fig. 1A). Moreover a correlation has been found between the Amu Darya runoff and the Indian Summer Monsoon, not due to spillover of monsoonal precipitation into the Amu Darya basin, but via tropospheric teleconnections leading to

temperature rise and glacier melting (Schiemann et al., 2007). Although debated at the moment (Chen et al., 2010), it is not impossible that the Indian Summer Monsoon penetrated further inland during the Early Holocene.

It is only recently that the glacial history of the western Himalayas has become better known owing to great improvements in dating techniques. The Pamir Mountains have had large glaciers during the first millennia of the Holocene (Owen, 2009). It is probable that these Early Holocene glaciers were the source of meltwater for the CS until 4 cal. ka BP. Hence, a low latitude forcing (via the Amu Darya and Uzboy) had become more important for a few millennia than the middle high latitudes one (Volga drainage basin).

5.3.5. The transition to the Neocaspian biozone

Only zone D-6 corresponds to the bottom-most zone Dz14-1 of the nearby core CP14 (Fig. 8), characterised in both cores by high values of *S. cruciformis* and *C. r. rugosum*.

The end of the Gousan highstand cannot be seen in the GS05 sequence but is well expressed in core CP14 (Fig. 8). A change from PC2-d positive to negative scores is detected at the Dz14-1/2 transition, ca 3.9 cal. ka BP (Fig. 7), pointing out more brackish conditions than in the previous freshwater phase.

It is from this moment that PC1-d shows positive and rising scores (Fig. 7). This principal component is difficult to interpret, but recent findings suggest that *L. machaerophorum* abundances could be reflecting water temperature increase (Leroy et al., 2013b).

The end of this highstand has also been identified in core TM (hiatus in core TM at c. 3.9 cal. ka BP, zones 4 to 5–6). It is suggested that these transitions in cores CP14 and core TM are driven by another lowstand (not severe enough to be identified in the deep sea core or at the time resolution of the current study) that marks the beginning of the Neocaspian biozone intermediate water levels.

5.4. Absence of direct links between vegetation and sea levels

Contrary to the few pollen spectra published for the Mangyshlak lowstand showing a dry period preceded and followed by a period with more arboreal pollen (Abramova and Mayev, 1974), the corresponding periods in core GS05 (P-4 and 5) show two dry periods with different characteristics (Fig. 8). This difference between studies is probably due to the higher sampling and time resolution of the present investigation.

The development of trees (zone P-6) in the surroundings of the CS is coeval to the start of the phase when the CS shows the freshest waters (zone D-6). The two phenomena may have occurred in a period of increased precipitation, corresponding to the Atlantic period of northern Europe.

Our results do not confirm the hypothesis that transgressions are linked to forest development and regression linked to arid phases (Kuprin and Rybakova, 2003). It seems that it is more subtle because different forcing factors are at play: changes in the palaeohydrographical network for the water level fluctuations (less directly linked to climate) and more directly changes in climate for terrestrial vegetation.

6. Conclusions

Beyond well circumscribed limitations of the chronological framework and the ecological interpretation of dinocyst assemblages dominated by new taxa, our results bearing on the first continuous sequence between the Allerød and 4.4 cal. ka BP in the Caspian region highlight rigorous, significant and original facts.

The Younger Dryas palynozone, first seen in the Caspian Sea region, is characterised by the development of a very arid desert-type vegetation. It is followed by 3100 years of a climate sufficiently dry to delay the development of trees around the Caspian Sea until 8.4 cal. ka BP. This is also reinforced by the fact that, in small areas of favourable microclimates, which played the role of glacial vegetation refugia (such as the foot of the Elburz Mountains), the development of trees occurred earlier, or even with no delay, at the early beginning of the Holocene. The highest palynological richness values are found between 8.4 and 4.4 cal. ka BP when the forest development was well under way. A small maximum is also detected during the Allerød, as some forest spread occurred. Thus, forest ecosystems in the area support higher diversities than steppe/desert ecosystems.

Dinoflagellate assemblages are for the first time available for the Mangyshlak lowstand. In the Early Holocene, the transition between a highstand and a lowstand, i.e. the Late Khvalynian and the Mangyshlak, is very likely caused by other drivers than local climatic change alone: a change in the palaeohydrology of the two main rivers, i.e. Volga and Amu Darya, must have occurred briefly and combined with the higher evaporation rates linked to Holocene warming.

Following the Mangyshlak lowstand and based on freshwater type dinocyst assemblages, a highstand is reconstructed with two successive phases reflecting increasingly freshwater. Until 4.4 ka BP ago at the latest (most likely until 3.9 cal. ka BP ago), the south basin had a high water level and was filled by relatively freshwater (3–7 psu) that could come not only from the melting of the Eurasian ice sheet anymore, but from also the Pamirs via the Amu Darya.

The present work re-emphasises that the high and lowstands, contrary to the world ocean, are not directly in line with glacial–interglacial periods, neither in phase, nor in anti-phase. However due to the rapidity of the past and present CS level changes and their vast economical impact, more efforts need to be made in solving dating problems and in the acquisition of a complete Holocene record.

Acknowledgements

This study has been conducted within the European Contract INCO-Copernicus “Understanding the Caspian Sea erratic fluctuations” n° IC15-CT96-0112. This was funded by the Centre National de la Recherche Scientifique within the framework of the INSU-DYTEC (DYnamique de la Terre et du Climat) Program (France). Thanks are due to the French and Russian colleagues, who organized and participated in the coring and hydrological sea expedition of August 1994. P.-J. Giannesini kindly provided the carbonate data and he and E. Moreno are the curators of the cores at the Museum National d’Histoire Naturelle de Paris, France. We are especially grateful to P. Tucholka and F. Guichard who actively contributed to the scientific part of this project. The publication is a contribution to the INQUA QuickLakeH project (No. 1227) and to the European project Marie Curie, CLIMSEAS-PIRSES-GA-2009-247512. Mr M. Turner (Brunel University) has kindly revised the English of the manuscript. LLM is funded by the Brunel IfE MINT Scheme.

References

Abramova, T.A., Mayev, E.G., 1974. Palynological characteristics and formation conditions of the horizon of the late-Khvalynian (Mangyshlak) regression of the Caspian Sea. In: Marine-palynological Researches in USSR, pp. 117–125 (in Russian).

Arpe, K., Bengtsson, L., Golitsyn, G.S., Mokhov, I.I., Semenov, V.A., Sporyshev, P.V., 2000. Connection between Caspian Sea level variability and ENSO. Geophys. Res. Lett. 27 (17), 2693–2696.

Arpe, K., Leroy, S.A.G., 2007. The Caspian Sea Level forced by the atmospheric circulation, as observed and modelled. Quat. Int. 173-174, 144–152.

Arpe, K., Leroy, S.A.G., Lahijani, H., Khan, V., 2012. Impact of the European Russia drought in 2010 on the Caspian Sea level. Hydrol. Earth Syst. Sci. 16, 19–27.

Arpe, K., Leroy, S.A.G., Mikolajewicz, U., 2011. A comparison of climate simulations for the last glacial maximum with three different versions of the ECHAM model and implications for summer-green tree refugia. Clim. Past 7, 91–114.

Arpe, K., Leroy, S.A.G., Wetterhall, F., Khan, V., Hagemann, S., Lahijani, H., 2013. Prediction of the Caspian Sea Level using ECMWF seasonal forecast and reanalysis. Theor. Appl. Climatol. online 14 August 2013 (in press).

Austin, P., Mackay, A., Palagushkina, O., Leng, M., 2007. A high-resolution diatom-inferred palaeoconductivity and lake level record of the Aral Sea for the last 1600 yr. Quat. Res. 67, 383–393.

Bahr, A., Lamy, F., Arz, H.W., Kuhlmann, H., Wefer, G., 2005. Late glacial to Holocene climate and sedimentation history in the NW Black Sea. Mar. Geol. 214 (4), 309–322.

Bennett, K., 2003. psimpoll and pscomb Programs for Plotting and Analysis. Version psimpoll 4.10 http://chrono.qub.ac.uk/psimpoll/psimpoll.html (last accessed 10.05.13.).

Blaauw, M., 2010. Methods and code for "classical" age-modelling of radiocarbon sequences. Quat. Geochronol. 5 (5), 512–518.

Bol'shakov, V.A., Vinogradov, Yu.K., Dara, O.M., Yanina, T.A., 2009. First results of investigation into relation between magnetic properties of bottom sediments in the Northern Caspian and variations in the Caspian Sea Level in the Late Neo-Pleistocene. Dokl. Akad. Nauk. 427 (5), 683–687.

Boomer, I., Aladin, N., Plotnikov, I., Whatley, R., 2000. The palaeolimnology of the Aral Sea: a review. Quat. Sci. Rev. 19, 1259–1278.

Bottema, S., 1995. The Younger Dryas in the Eastern Mediterranean. Quat. Sci. Rev. 14, 883–891.

Bradley, L., Marret, F., Mudie, P., Aksu, A., Hiscott, R., 2012. Constraining Holocene sea-surface conditions in the southwestern Black Sea using dinoflagellate cysts. J. Quat. Sci. 27 (8), 835–843.

Chalié, F., the Caspian Sea INSU-DYTEC Program Members, Escudié, A.S., Badaut-Trauth, D., Blanc, G., Blanc-Valleron, M.M., Brigault, S., Desprairies, A., Ferronsky, V.I., Giannesini, P.J., Gibert, E., Guichard, F., Jelinowska, A., Massault, M., Mélières, F., Tribovilllard, N., Tucholka, P., Gasse, F., 1997. The glacial-post glacial transition in the southern Caspian Sea. In: Comptes Rendus de l'Académie des Sciences Paris, série 2a 324, serie IIa, pp. 309–316.

Chen, F.-H., Chen, J.-H., Holmes, J., Boomer, I., Austin, P., Gates, J.B., Wang, N.-L., Brooks, S.J., Zhang, J.-W., 2010. Moisture changes over the last millennium in arid central Asia: a review, synthesis and comparison with monsoon region. Quat. Sci. Rev. 29, 1055–1068.

Chepalyga, A.L., 2007. The late glacial Great Flood in the Ponto-Caspian basin. In: Yanko-Hombach, V., Gilbert, A.S., Panin, N., Dolukhanov, P. (Eds.), The Black Sea Flood Question: Changes in Coastline, Climate and Human Settlement. Springer, pp. 119–148.

Connor, S.E., 2006. A Promethean Legacy: Late Quaternary Vegetation History of Southern Georgia, Caucasus (PhD thesis). University of Melbourne, Australia.

Desprat, S., Combourieu-Nebout, N., Essallami, L., Sicre, M.A., Dormoy, I., Peyron, O., Siani, G., Bout Roumazeilles, V., Turon, J.L., 2013. Deglacial and Holocene vegetation and climatic changes in the southern Central Mediterranean from a direct land–sea correlation. Clim. Past 9, 767–787.

Djamali, M., Baumel, A., Brewer, S., Jackson, S.T., Kadereit, J.W., López-Vinyallonga, S., Mehregan, I., Shabanian, E., Simakova, A., 2012. Ecological implications of Cousinia Cass (Asteraceae) persistence through the last two glacial–interglacial cycles in the continental Middle East for the Irano-Turanian flora. Rev. Palaeobot. Palynol. 172, 10–20.

Djamali, M., Beaulieu, J.L., Shah-hosseini, M., Andrieu-Ponel, V., Ponel, P., Amini, A., Akhani, H., Leroy, S.A.G., Stevens, L., Lahijani, H., Brewer, S., 2008. A late Pleistocene long pollen record from Lake Urmia, NW Iran. Quat. Res. 69, 413–420.

Djamali, M., Miller, N.F., Ramezani, E., Akhani, H., Andrieu- Ponel, V., de Beaulieu, J.-L., Berberian, M., Guibal, F., Lahijani, H., Lak, R., Ponel, P., 2011. Notes on the arboricultural and agricultural practices in ancient Iran based on new pollen evidence. Paléorient 36.2, 175–188.

Dumont, H.J., 1998. The Caspian Lake: history, biota, structure, and function. Limnol. Oceanogr. 43 (1), 44–52.

Escudié, A.-S., Blanc, G., Chalié, F., Clauer, N., Filly, A., Gibert, E., Massault, M., Mélières, F., Van Exter, S., Zuppi, G.M., Gasse, F., 1998. Understanding present and past Caspian Sea evolution. Contribution from isotope tracers. In: Study of Past and Current Environmental Changes in the Hydrosphere and the Atmosphere. Proceedings of an International Symposium on Isotope Techniques Organised by the IAEA, pp. 623–631. Vienna, STI/PUB/1024.

Ferronsky, V.I., Polyakov, V.A., Kuprin, P.N., Lobov, A.L., 1999. The nature of variations in the level of the Caspian Sea (based on bottom-sediment data). Water Resour. 26 (6), 583–596.

Filipova-Marinova, M., Pavlov, D., Coolen, M., Giosan, L., 2013. First high-resolution marinopalynological stratigraphy of Late Quaternary sediments from the central part of the Bulgarian Black Sea area. Quat. Int. 293, 170–183.

Fontes, J.C., Mélières, F., Gibert, E., Qing, Liu, Gasse, F., 1993. Stable isotope and radiocarbon balances of two Tibetan lakes (Sumxi Co, Longmu Co) from 13,000 BP. Quat. Sci. Rev. 12, 875–887.

Forte, A.M., Cowgill, E., 2013. Late Cenozoic base-level variations of the Caspian Sea: a review of its history and proposed driving mechanisms. Palaeogeogr. Palaeoclimatol. Palaeoecol. 386 (15), 392–407.

Froehlich, K., Rozanski, K., Povinec, P., Oregioni, B., Gastaud, J., 1999. Isotope studies in the Caspian Sea. Sci. Total Environ. 237-238, 419–427.

Grigorovich, I.A., Therriault, T.W., MacIsaac, H.J., 2003. History of aquatic invertebrate invasions in the Caspian Sea. Biol. Invasions 5, 103–115.

Grosswald, M., 1993. Extent and melting history of the late Weichselian ice sheet, the Barents-Kara continental margin. In: Peltier, W.R. (Ed.), Ice in the Climate System. Springer Verlag Berlin, pp. 1–20. NATO ASI Series, I 12.

Hammer, Ø., Harper, D.A.T., Ryan, P.D., 2001. PAST: paleontological statistics software package for education and data analysis. Palaeontol. Electron. 4 (1), 9.

Hiscott, R.N., Aksu, A.E., Mudie, P.J., Marret, F., Abrajano, T., Kaminski, M.A., Evans, J., Çakıroğlu, A.I., Yaşar, D., 2007. A gradual drowning of the southwestern Black Sea shelf: evidence for a progressive rather than abrupt Holocene reconnection with the eastern Mediterranean Sea through the Marmara Sea Gateway. Quat. Int. 167–168, 19–34.

Hoogendoorn, R.M., Levchenko, O., Missiaen, T., Lychagin, M., Richards, K., Gorbunov, A., Kasimov, N., Kroonenberg, S.B., 2010. High resolution seismic stratigraphy of the modern Volga Delta, Russia. In: Proceedings of the International Conference "The Caspian Region: Environmental Consequences of the Climate Change", October 14–16, 2010. Moscow Sate University, Faculty of Geography, pp. 32–37 (Extended abstract) http://media.geogr.msu.ru/Caspian_2010/caspian_conference_2010.pdf (last accessed 09.08.13.).

Jelinowska, A., Tucholka, P., Badaut-Trauth, D., 1999. Magnetic mineral variations of south Caspian Sea sediments at the laminae scale. Phys. Chem. Earth (A) 24 (9), 823–828.

Jelinowska, A., Tucholka, P., Guichard, F., Lefèvre, I., Badaut-Trauth, D., Chalié, F., Gasse, F., Tribovillard, N., Desprairies, A., 1998. Mineral magnetic study of Late Quaternary South Caspian Sea sediments: paleoenvironmental implications. Geophys. J. Int. 133, 499–509.

Kakroodi, A.A., Kroonenberg, S.B., Hoogendoorn, R.M., Mohammed Khani, H., Yamani, M., Ghassemi, M.R., Lahijani, H.A.K., 2012. Rapid Holocene sea-level changes along the Iranian Caspian coast. Quat. Int. 263, 93–103.

Kazancı, N., Gulbabazadeh, T., Leroy, S.A.G., Ileri, O., 2004. Sedimentary and environmental characteristics of the Gilan-Mazenderan plain, northern Iran: influence of long- and short-term Caspian water level fluctuations on geomorphology. J. Mar. Syst. 46 (1–4), 145–168.

Kes, A.S., 1995. Chronicle of the Aral Sea and the sub-aral region. GeoJournal 35 (1), 7–10.

Kideys, A.E., Soydemir, N., Eker, E., Vladymyrov, V., Soloviev, D., Melin, F., 2005. Phytoplankton distribution in the Caspian Sea during March 2001. Hydrobiologia 543, 159.

Kosarev, A.N., Yablonskaya, E.A., 1994. The Caspian Sea. SPB Academic Publishing, The Hague.

Kroonenberg, S.B., Rusakov, G.V., Svitoch, A.A., 1997. The wandering of the Volga delta: a response to rapid Caspian sea-level change. Sedim. Geol. 107, 189–209.

Kuprin, P.N., Ferronsky, V.I., Popovchak, V.P., Shlykov, V.G., Zolotaya, L.A., Kalisheva, M.V., 2003. Bottom sediments of the Caspian Sea as an indicator of changes in its water regime. Water Resour. 30 (2), 136–153.

Kuprin, P.N., Pirumova, L.G., 2002. Synchronous changes in the diatom complexes and hydrological conditions in the Middle and Southern Caspian paleobasins. Water Resour. 29 (6), 605–621.

Kuprin, P.N., Rybakova, N.O., 2003. Analysis of palynological complexes of deep-Sea sediments in the Middle and Southern Caspian. Water Resour. 30 (1), 1–9.

Kuprin, P.N., Zolotaya, L.A., Kalisheva, M.V., 2002. Magnetic susceptibility of deep-water sediments of the South and Middle Caspian Sea. Lithol. Mineral Resour. 37 (4), 364–373.

Kuzmin, Y.V., Nevesskaya, L.A., Krivonogov, S.K., Burr, G.S., 2007. Apparent ^{14}C ages of the 'pre-bomb' shells and correction values (R, ΔR) for Caspian and Aral Seas (Central Asia). Nucl. Instrum. Methods Phys. Res. Sect. B 259, 463–466.

Lahijani, H., Tavakoli, V., 2012. Identifying provenance of South Caspian coastal sediments using mineral distribution pattern. Quat. Int. 261, 128–137.

Lambeck, K., 1996. Limits on the areal extent of the Barents Sea ice sheet in late Weichselian time. Glob. Planet. Ch 12, 41–51.

Leroy, S.A.G., 2010. Palaeoenvironmental and Palaeoclimatic Changes in the Caspian Sea Region Since the Lateglacial from Palynological Analyses of Marine Sediment Cores. Geography, Environment, Sustainability, Faculty of Geography of Lomonosov Moscow State University and by the Institute of Geography of RAS. 2, pp. 32–41.

Leroy, S.A.G., Albay, M., 2010. Palynomorphs of brackish and marine species in cores from the freshwater Lake Sapanca, NW Turkey: further evidence of palaeo-contacts with the Black Sea? Rev. Palaeobot. Palynol. 160 (3–4), 181–188.

Leroy, S.A.G., Arpe, K., 2007. Glacial refugia for summer-green trees in Europe and S-W Asia as proposed by ECHAM3 time-slice atmospheric model simulations. J. Biogeogr. 34, 2115–2128.

Leroy, S.A.G., Kakroodi, A.A., Kroonenberg, S.B., Lahijani, H.A.K., Alimohammadian, H., Nigarov, A., 2013a. Holocene vegetation history and sea level changes in the SE corner of the Caspian Sea: relevance to SW Asia climate. Quat. Sci. Rev. 70, 28–47.

Leroy, S.A.G., Lahijani, H.A.K., Djamali, M., Naqinezhad, A., Moghadam, M.V., Arpe, K., Shah-Hosseini, M., Hosseindoust, M., Miller, Ch.S., Tavakoli, V., Habibi, P., Naderi, M., 2011. Late Little Ice Age palaeoenvironmental records from the Anzali and Amirkola lagoons (south Caspian Sea): vegetation and sea level changes. Palaeogeogr. Palaeoclimatol. Palaeoecol. 302, 415–434.

Leroy, S.A.G., Lahijani, H.A.K., Reyss, J.-L., Chalié, F., Haghani, S., Shah-Hosseini, M., Shahkarami, S., Tudryn, A., Arpe, K., Habibi, P., Nasrollahzadeh, H.S., Makhlough, A., 2013b. A two-step expansion of the dinocyst *Lingulodinium machaerophorum* in the Caspian Sea: the role of changing environment. Quat. Sci. Rev. 77, 31–45.

Leroy, S.A.G., Marret, F., Gibert, E., Chalié, F., Reyss, J.-L., Arpe, K., 2007. River inflow and salinity changes in the Caspian Sea during the last 5500 years. Quat. Sci. Rev. 26, 3359–3383.
Leroy, S.A.G., Marret, F., Giralt, S., Bulatov, S.A., 2006. Natural and anthropogenic rapid changes in the Kara-Bogaz Gol over the last two centuries by palynological analyses. Quat. Int. 150, 52–70.
Leroy, S.A.G., Roiron, P., 1996. Final Pliocene macro and micro floras of the paleovalley of Bernasso (Escandorgue, France). Rev. Palaeobot. Palynol. 94, 295–328.
Létolle, R., 2000. Histoire de l'Ouzboï, cours fossile de l'Amou Darya synthèse et éléments nouveaux. Studia Iranica 29 (2), 195–240.
Levin, I., Graul, R., Trivett, N.B.A., 1995. Long-term observations of atmospheric CO_2 and carbon isotopes at continental sites in Germany. Tellus 47B, 23–34.
Londeix, L., Herreyre, Y., Turon, J.-L., Fletcher, W., 2009. Last Glacial to Holocene hydrology of the Marmara Sea inferred from a dinoflagellate cyst record. Rev. Palaeobot. Palynol. 158, 52–71.
Mamedov, A.V., 1997. The Late Pleistocene–Holocene history of the Caspian Sea. Quat. Int. 41-42, 161–166.
Mangerud, J., Astakhov, V., Jakobsson, M., Svendsen, J., 2001. Huge ice-age lakes in Russia. J. Quat. Sci. 16 (8), 773–777.
Marret, F., Leroy, S.A.G., Chalié, F., Gasse, F., 2004. New organic-walled dinoflagellate cysts from recent sediments of central Asian seas. Rev. Palaeobot. Palynol. 129, 1–20.
Marret, F., Zonneveld, K.A.F., 2003. Atlas of modern organic-walled dinoflagellate cyst distribution. Rev. Palaeobot. Palynol. 125, 1–200.
Mayev, E.G., 2010. Mangyshlak regression of the Caspian Sea: relationship with climate. In: Proceedings of the International Conference —The Caspian Region: Environmental Consequences of the Climate Change. October, 14–16, Moscow, Russia. Faculty of Geography, Moscow, pp. 107–109.
McCarthy, F.M.G., Mudie, P.J., 1998. Oceanic pollen transport and pollen: dinocyst ratios as markers of late Cenozoic sea level change and sediment transport. Palaeogeogr. Palaeoclimatol. Palaeoecol. 138, 187–206.
Mertens, K.N., Ribeiro, S., Bouimetarhan, I., Caner, H., Combourieu-Nebout, N., Dale, B., de Vernal, A., Ellegaard, M., Filipova, M., Godhe, A., Goubert, E., Grøsfjeld, K., Holzwarth, U., Kotthoff, U., Leroy, S.A.G., Londeix, L., Marret, F., Matsuoka, K., Mudie, P.J., Naudts, L., Peña-Manjarrez, J.L., Persson, A., Popescu, S.-M., Pospelova, V., Sangiorgi, F., van der Meer, M., Vink, A., Zonneveld, K.A.F., Vercauteren, D., Vlassenbroeck, J., Louwye, S., 2009. Process length variation in cysts of a dinoflagellate, *Lingulodinium machaerophorum*, in surface sediments: investigating its potential as salinity proxy. Mar. Micropal. 70, 54–69.
Mudie, P.J., Leroy, S.A.G., Marret, F., Gerasimenko, N., Kholeif, S.E.A., Sapelko, T., Filipova-Marinova, M., 2011. Non-pollen palynomorphs: indicators of salinity and environmental change in the Caspian-Black Sea-Mediterranean corridor. In: Buynevich, I., Yanko-Hombach, V., Gilbert, A.S., Martin, R.E. (Eds.), Geology and Geoarchaeology of the Black Sea Region: Beyond the Flood Hypothesis, Geological Society of America Special Paper 473, pp. 89–115.
Mudie, P.J., Rochon, A., Aksu, A.E., Gillespie, H., 2002. Dinoflagellate cysts, freshwater algae and fungal spores as salinity indicators in Late Quaternary cores from Marmara and Black seas. Mar. Geol. 190, 203–231.
Muscheler, R., Kromer, B., Björck, S., Svensson, A., Friedrich, M., Kaiser, K.F., Southon, J., 2008. Tree rings and ice cores reveal ^{14}C calibration uncertainties during the Younger Dryas. Nat. Geosci. 1 (4), 263–267.
Naderi Beni, A., Lahijani, H., Mousavi Harami, R., Arpe, K., Leroy, S.A.G., Marriner, N., Berberian, M., Ponel, V.A., Djamali, M., Mahboubi, A., Reimer, P.J., 2013. Caspian sea level changes during the last millennium: historical and geological evidences from the south Caspian Sea. Clim. Past 9, 1645–1665.
Owen, L.A., 2009. Latest Pleistocene and Holocene glacier fluctuations in the Himalaya and Tibet. Quat. Sci. Rev. 28, 2150–2164.
Pierret, M.-C., Chabaux, F., Leroy, S.A.G., Causse, C., 2012. A record of Late Quaternary continental weathering in the sediment of the Caspian Sea: evidence from U-Th, Sr isotopes, trace element and palynological data. Quat. Sci. Rev. 51, 40–55.
Räsänen, J., Kauppila, T., Vuorio, K., 2006. Sediment and phytoplankton records of the cyanobacterial genus *Anabaena* in boreal Lake Pyhajarvi. Hydrobiology 568, 455–465.
Reille, M., 1992. Pollen et Spores d'Europe et d'Afrique du Nord. Laboratoire de Botanique Historique et Palynologie, CNRS, Marseille.
Reille, M., 1995. Pollen et spores d'Europe et d'Afrique du Nord, Supplément 1. Laboratoire de botanique historique et de palynologie, Marseille.
Reille, M., 1998. Pollen et spores d'Europe et d'Afrique du Nord, Supplément 2. Laboratoire de botanique historique et de palynologie, Marseille.
Reimer, P.J., Baillie, M.G.L., Bard, E., Bayliss, A., Beck, J.W., Blackwell, P.G., Bronk Ramsey, C., Buck, C.E., Burr, G.S., Edwards, R.L., Friedrich, M., Grootes, P.M., Guilderson, T.P., Hajdas, I., Heaton, T.J., Hogg, A.G., Hughen, K.A., Kaiser, K.F., Kromer, B., McCormac, F.G., Manning, S.W., Reimer, R.W., Richards, D.A., Southon, J.R., Talamo, S., Turney, C.S.M., van der Plicht, J., Weyhenmeyer, C.E., 2009. IntCal09 and Marine09 radiocarbon age calibration curves, 0–50,000 years cal BP. Radiocarbon 51, 1111–1150.
Rekacewicz, P., 2007a. http://www.grida.no/graphicslib/detail/caspian-sea-salinity_829b (last accessed 10.05.13.).
Rekacewicz, P., 2007b. http://www.grida.no/graphicslib/detail/mean-sea-surface-temperature_eeff (last accessed 10.05.13.).
Richardson, S.E.J., Davies, R.J., Allen, M.B., Grant, S.F., 2011. Structure and evolution of mass transport deposits in the South Caspian Basin, Azerbaijan. Basin Res. 23, 702–719.
Rodionov, S.N., 1994. Global and Regional Climatic Interaction: the Caspian Sea Experience. Kluwer Academic Press, Dordrecht.
Ryan, W.B.F., Major, C.O., Lericolais, G., Goldstein, St.L., 2003. Catastrophic flooding of the Black Sea. Annu. Rev. Earth Planet. Sci. 31, 525–556.
Rychagov, G.I., 1997. Holocene oscillations of the Caspian Sea and forecasts based on palaeogeographical reconstructions. Quat. Int. 41-42, 167–172.
Schiemann, R., Glazirina, M.G., Schär, C., 2007. On the relationship between the Indian summer monsoon and river flow in the Aral Sea basin. Geophys. Res. Lett. 34, L05706.
Shiklomanov, I.A., Georgievsky, V.Y., Kopaliani, Z.D., 1995. Water balance of the Caspian Sea and reasons of water level rise in the Caspian Sea. In: UNESCO (Ed.), UNESCO-IHP-IOC-IAEA Workshop on Sea Level Rise and the Multidisciplinary Studies of Environmental Processes in the Caspian Sea Region, Intergovernmental Oceanographic Commission, pp. 1–27. Workshop Report N°108-Supplément, Paris (France).
Shumilovskikh, L.S., Marret, F., Fleitmann, D., Arz, H.W., Nowaczyk, N., Behling, H., 2013. Eemian and Holocene sea-surface conditions in the southern Black Sea: organic-walled dinoflagellate cyst record from core 22-GC3. Mar. Micropal. 101, 146–160.
Shumilovskikh, L.S., Tarasov, P., Arz, H.W., Fleitmann, D., Marret, F., Nowaczyk, N., Plessen, B., Schultz, F., Behling, H., 2012. Vegetation and environmental dynamics in the southern Black Sea region since 18 kyr BP derived from the marine core 22-GC3. Palaeogeogr. Palaeoclimatol. Palaeoecol. 337-338, 177–193.
Sidorchuk, A.Yu., Panin, A.V., Borisova, O.K., 2009. Morphology of river channels and surface runoff in the Volga River basin (East European plain) during the Late Glacial period. Geomorphology 113, 137–157.
Small, E.E., Sloan, L.C., Nychka, D., 2001. Changes in surface air temperature caused by desiccation of the Aral Sea. J. Clim. 14 (3), 284–299.
Sorokin, V.M., 2011. Correlation of Upper Quaternary deposits and Paleogeography of the Black and Caspian Seas. Stratigr. Geol. Correl. 19 (5), 563–578.
Sorrel, P., Popescu, S.-M., Head, M.J., Suc, J.-P., Klotz, S., Oberhänsli, H., 2006. Hydrographic development of the Aral Sea during the last 2000 years based on a quantitative analysis of dinoflagellate cysts. Palaeogeogr. Palaeoclimatol. Palaeoecol. 234, 304–327.
Svitoch, A.A., 2009. Khvalynian transgression of the Caspian Sea was not a result of water overflow from the Siberian Proglacial lakes, nor a prototype of the Noachian flood. Quat. Int. 197, 115–125.
Svitoch, A.A., 2010. The Neoeuxinian basin of the Black Sea and the Khvalinian transgression of the Caspian Sea. Quat. Int. 225, 230–234.
Svitoch, A.A., 2012. The Caspian Sea Shelf during the Pleistocene regressive Epochs. Oceanology 52 (4), 526–539.
Syed, F.S., Giorgi, F., Pal, J.S., King, M.P., 2006. Effect of remote forcings on the winter precipitation of central southwest Asia part 1: observations. Theor. Appl. Climatol. 86, 147–160.
Tudryn, A., Giannesini, P.-J., Guichard, F.O., Badaut-Trauth, D., Tucholka, P., Boomer, I., 2013. The role of iron minerals in laminae formation in Late Pleistocene sediments of the Caspian Sea. Quat. Int. 292, 193–204.
UNEP, GRID, ZOI, 2011. Environment and Security in the Amu Darya Basin. http://capacity4dev.ec.europa.eu/system/files/file/10/01/2013_-_1505/environment_and_security_in_the_amu_darya_basin.pdf (last accessed 12.05.13.).
USDA, 2013. Caspian Sea Heights Variations. http://www.pecad.fas.usda.gov/cropexplorer/global_reservoir/gr_regional_chart.aspx?regionid=stans&reservoir_name=Caspian (last accessed 01.05.13.).
Valsecchi, V., Sánchez-Goñi, M.F., Londeix, L., 2012. Vegetation dynamics in the Northeastern Mediterranean region during the past 23 000 yr: insights from a new pollen record from the Sea of Marmara. Clim. Past 8, 1941–1956.
Vincent, S.J., Davies, C.E., Richards, K., Aliyeva, E., 2010. Contrasting Pliocene fluvial depositional systems within the rapidly subsiding South Caspian Basin; a case study of the palaeo-Volga and palaeo-Kura river systems in the Surakhany Suite, Upper Productive Series, onshore Azerbaijan. Mar. Pet. Geol. 27, 2079–2106.
Wall, D., Dale, B., Harada, K., 1973. Descriptions of new fossil dinoflagellates from the Late Quaternary of the Black Sea. Micropaleontology 19 (1), 18–31.
Walter, H., Breckle, S.-W., 1989. Temperate and Polar Zonobiomes of Northern Eurasia. Springer, Berlin.
Weinstein, A., 1989. Provenance evaluation of *Pinus halepensis*, *P. brutia* and *P. eldarica* in Israel. For. Ecol. Manage. 26, 215–225.
Wright, H.E., Ammann, B., Stefanova, I., Atanassova, J., Margalitadze, N., Wick, L., Blyakharchuk, T., 2003. Late-Glacial and Early-Holocene dry climates from the Balkan Peninsula to southern Siberia. In: Tonkov, S. (Ed.), Aspects of Palynology and Palaeoecology. PENSOFT Publishers, Sofia-Moscow, pp. 127–136.
Zenkevitch, L.A., 1963. Biology of the Seas of the USSR. George Allen and Unwin Ltd, London.